Comparative interactomes of HSF1 in stress and disease reveal a role for CTCF in HSF1-mediated gene regulation

Received for publication, August 3, 2020, and in revised form, November 10, 2020 Published, Papers in Press, November 18, 2020,
https://doi.org/10.1074/jbc.RA120.015452

Eileen T. Burchfiel[1,2], Anniina Vihervaara[3], Michael J. Guertin[4], Rocio Gomez-Pastor[2], and Dennis J. Thiele[1,2,5,*]

From the Departments of [1]Biochemistry and [2]Pharmacology and Cancer Biology, Duke University School of Medicine, Durham, North Carolina, USA; [3]Department of Molecular Biology and Genetics, Cornell University, Ithaca, New York, USA; [4]Department of Biochemistry and Molecular Genetics, University of Virginia, Charlottesville, Virginia, USA; and [5]Department of Molecular Genetics and Microbiology, Duke University School of Medicine, Durham, North Carolina, USA

Edited by Ursula Jakob

Heat shock transcription factor 1 (HSF1) orchestrates cellular stress protection by activating or repressing gene transcription in response to protein misfolding, oncogenic cell proliferation, and other environmental stresses. HSF1 is tightly regulated via intramolecular repressive interactions, post-translational modifications, and protein-protein interactions. How these HSF1 regulatory protein interactions are altered in response to acute and chronic stress is largely unknown. To elucidate the profile of HSF1 protein interactions under normal growth and chronic and acutely stressful conditions, quantitative proteomics studies identified interacting proteins in the response to heat shock or in the presence of a poly-glutamine aggregation protein cell-based model of Huntington's disease. These studies identified distinct protein interaction partners of HSF1 as well as changes in the magnitude of shared interactions as a function of each stressful condition. Several novel HSF1-interacting proteins were identified that encompass a wide variety of cellular functions, including roles in DNA repair, mRNA processing, and regulation of RNA polymerase II. One HSF1 partner, CTCF, interacted with HSF1 in a stress-inducible manner and functions in repression of specific HSF1 target genes. Understanding how HSF1 regulates gene repression is a crucial question, given the dysregulation of HSF1 target genes in both cancer and neurodegeneration. These studies expand our understanding of HSF1-mediated gene repression and provide key insights into HSF1 regulation via protein-protein interactions.

Organisms are constantly challenged with adapting to stressful conditions such as protein misfolding, inflammation, environmental toxicants, increased temperature, and rapid cell proliferation. A crucial player in the cellular stress response is heat shock transcription factor 1 (HSF1), a regulator of stress-protective gene transcription (1–4). In normal cells in the absence of acute stress, the majority of HSF1 is maintained in an inactive, monomeric state and resides predominantly in the cytoplasm (5, 6). This basal repression of HSF1 is achieved through protein interactions including a multichaperone complex (7–12), proteins that post-translationally modify HSF1, and repressive intramolecular interactions between leucine zipper regions (13–17). HSF1 is activated in response to stressful conditions through oligomerization and is retained in the nucleus where it binds heat shock elements (HSEs) adjacent to target genes or in distal regulatory elements to promote cell survival through several mechanisms (1, 2). Genes activated by HSF1 encode protein chaperones, the ubiquitin proteasome degradation machinery, cell cycle determinants, transcriptional regulators, and many other proteins involved in diverse processes (3). A more recently explored facet of HSF1 biology is its role in repressing gene transcription, including those involved in apoptosis, inflammation, and transcription (18–22).

Although HSF1 is primarily cytosolic and inactive in the absence of stress, a small fraction of HSF1 remains in the nucleus and binds to target genes in the absence of acute stress (23, 24). The characterization of HSF1 direct target genes in basal conditions and in response to acute stress, chronic protein misfolding diseases, or in cancer cells reveals cell-context-specific sets of HSF1-regulated genes, some of which contribute to pathogenesis (24–28). How HSF1 protein regulators are altered to influence different disease signatures is not well understood.

Owing to the central role HSF1 plays in coping with stresses that disrupt protein homeostasis, HSF1 is of great interest in neurodegenerative diseases that arise from chronic protein misfolding including Alzheimer's disease, Parkinson's disease, and Huntington's disease (HD) (5, 29–33). In HD, a CAG triplet nucleotide expansion in exon 1 of the Huntingtin gene results in a pathogenic polyglutamine (polyQ) expansion in the Htt protein (mutant Htt, mHtt) (34). mHtt protein aggregates in complexes with cellular components including cell signaling

This article contains supporting information.

* For correspondence: Dennis J. Thiele, dthiele@sisupharma.com.
Present address for Anniina Vihervaara: Institute of Biotechnology, University of Helsinki, Helsinki, Finland.
Present address for Rocio Gomez-Pastor: Department of Neuroscience, University of Minnesota, Minneapolis, Minnesota, USA.
Present address for Dennis J. Thiele: Sisu Pharma, Inc, Durham, North Carolina, USA.

proteins, transcription factors, and other key regulatory proteins, disrupting cellular function and ultimately increasing the propensity for apoptosis (35, 36). The protein misfolding and cellular dysfunction is further exacerbated by reduced levels of protein quality control (QC) components, including protein chaperones and the protein degradation machinery, which aid in maintaining protein homeostasis. Consequently, activation of cytoprotective protein chaperones such as Hsp70 and Hsp40, the TRiC chaperonin subunits, and the protein degradation machinery alleviates protein misfolding and augments aggregate clearance in HD (37–41). Furthermore, activation of multiple chaperone systems via HSF1 is more efficacious than a single chaperone (37–41) as HSF1 simultaneously elevates levels of protein QC components and regulates target genes to promote protein homeostasis and cell survival; thus, HSF1 activation is a promising point of therapeutic intervention (1, 3, 5, 33, 42–44). However, in response to mHtt, this stress-protective transcription factor is aberrantly degraded, its target gene expression blunted, and its genome-wide binding dramatically altered, raising questions of how HSF1 is dysregulated in HD (28, 29, 31, 33). A more detailed understanding of the regulation of HSF1 in unstressed cells, the dysfunctional regulation of HSF1 in HD, and how this compares with the acute stress of heat shock (HS) may offer new insights into HSF1 regulation and its contribution to disease.

Previous studies conducted in HD cellular and mouse models revealed that the impairment of HSF1 arises, in part, from inappropriate protein interactions that result in HSF1 degradation (33). In HD, elevated expression of protein kinase CK2α' and E3 ligase component FBXW7 promote the phosphorylation-dependent degradation of HSF1 (33). In contrast to the elevated HSF1 degradation in HD, compromised FBXW7 function in cancers impairs HSF1 degradation, giving rise to increased HSF1 protein levels that support malignancy (45–48).These and other studies demonstrate the importance of protein-protein interactions in modulating HSF1 nuclear retention, DNA binding, activation or repression of target genes, and degradation (8, 10, 22, 49–52). For instance, mitochondrial single-stranded DNA-binding protein is crucial for the activation of some HSF1 target genes in response to elevated temperatures (51). BCL2-associated athanogene 3 (BAG3) regulates HSF1 nuclear retention during heat stress (49), whereas RPA70 facilitates basal HSF1 binding at the Hsp70 locus by recruiting histone chaperone FACT (50). In addition to illuminating regulatory mechanisms imposed on HSF1 by interacting proteins, the study of other protein interactors has revealed roles for HSF1 in new pathways, including DNA repair (53, 54), metabolism (55), and the mitochondrial unfolded protein response (56). Taken together, these and other studies demonstrate how protein regulators of HSF1 can significantly alter HSF1 activity, function, and degradation. However, many of these regulatory interactions have been explored exclusively in response to heat shock, highlighting the need for a systematic proteomics approach in which the HSF1 interactome can be simultaneously investigated under different stress conditions, including chronic protein misfolding.

To decipher new aspects of HSF1 regulation via protein partners under distinct cellular stress states, the HSF1 interactome was examined during normal growth conditions, acute heat shock, and the chronic protein misfolding stress encountered in HD. HSF1 interacts with an array of proteins with diverse cellular functions, including mRNA processing, chromatin modification, transcriptional coactivators and repressors, and DNA and RNA metabolism. Although some of these interactions are maintained under all conditions evaluated, HSF1 also interacts with a distinct network of protein partners during acute versus chronic stress. CCCTC-binding protein (CTCF) was identified as an HSF1 interactor under all three conditions. CTCF and HSF1 interact *in vivo* and directly *in vitro*; this interaction requires the DNA-binding domain (DBD) of HSF1 but does not require HSF1 to be DNA binding competent. Acute depletion of CTCF or HSF1 reveals a strong overlap of potential repression targets and, given the co-occupancy of CTCF and HSF1 at genomic loci (26), indicate that CTCF may help recruit HSF1 and facilitate HSF1-mediated regulation of gene targets. This potential cooperation between HSF1 and CTCF could reveal a novel mechanism for HSF1-mediated target gene regulation, particularly for HSF1 repression targets.

Results

HSF1-interacting proteins in control, heat shock, and Huntington's disease model cells

To identify proteins that interact with HSF1 in cells during normal growth conditions, in response to the acute stress of heat shock, or during the chronic stress of protein misfolding of HD, endogenous HSF1 was immunoprecipitated and interacting proteins were identified using mass spectrometry. Striatal neuron-derived cells from HD model mice possessing pathogenic polyQ-expanded Htt, STHdh$^{Q111/Q111}$ (Q111, HD), were compared with their wildtype counterpart, STHdh$^{Q7/Q7}$ (Q7, Control) (57). This well-characterized HD cell model recapitulates several phenotypes of HD including cellular dysfunction, aberrant localization of mHtt protein, and compromised HSF1 DNA binding and target gene expression (28, 31, 57).

To enable the identification of protein interactions with HSF1 present at physiologically relevant levels in the absence of a cross-linking agent, endogenous, native, and untagged HSF1 was immunoprecipitated and interacting proteins were identified with mass spectrometry. This is significant because HSF1 overexpression drives unnatural oligomerization and DNA binding, which could result in protein interactions that are not relevant at physiological levels of HSF1 (58). In addition, as HSF1 levels are diminished in HD owing to aberrant protein modifications and interactions, overexpression may alter the specific HSF1 interactions (33, 59). Immunoprecipitated HSF1 or negative control IgG precipitates were analyzed by ultraperformance liquid chromatography tandem-mass spectrometry (LC-MS/MS), and the HSF1 interactome was quantitatively assessed in unstressed conditions and during acute and chronic stress (Fig. 1*A*). HSF1-interacting proteins

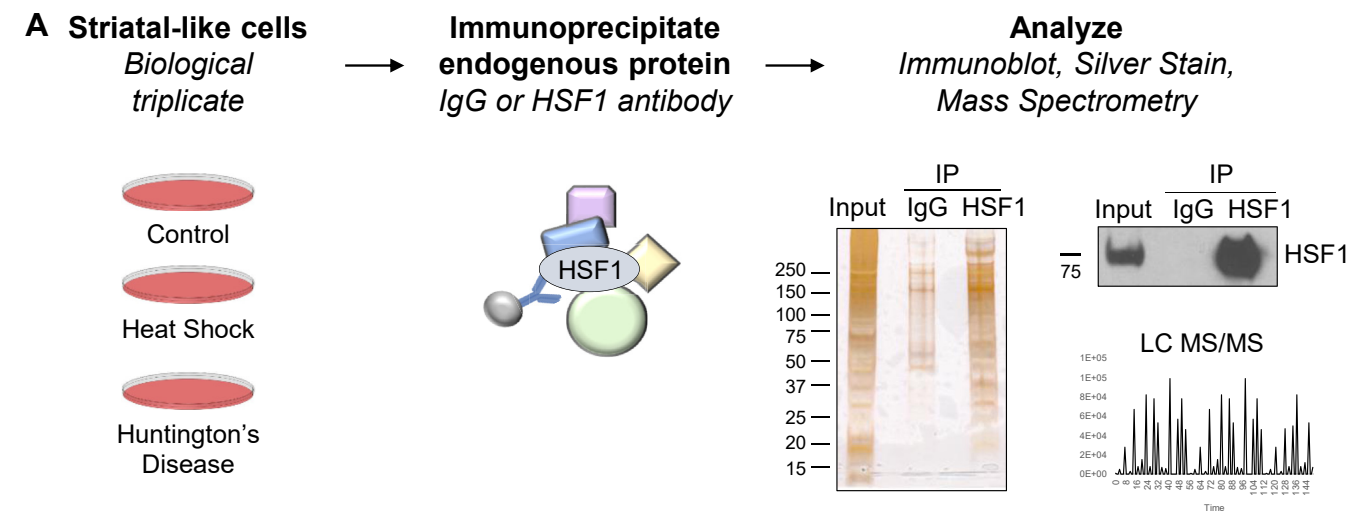

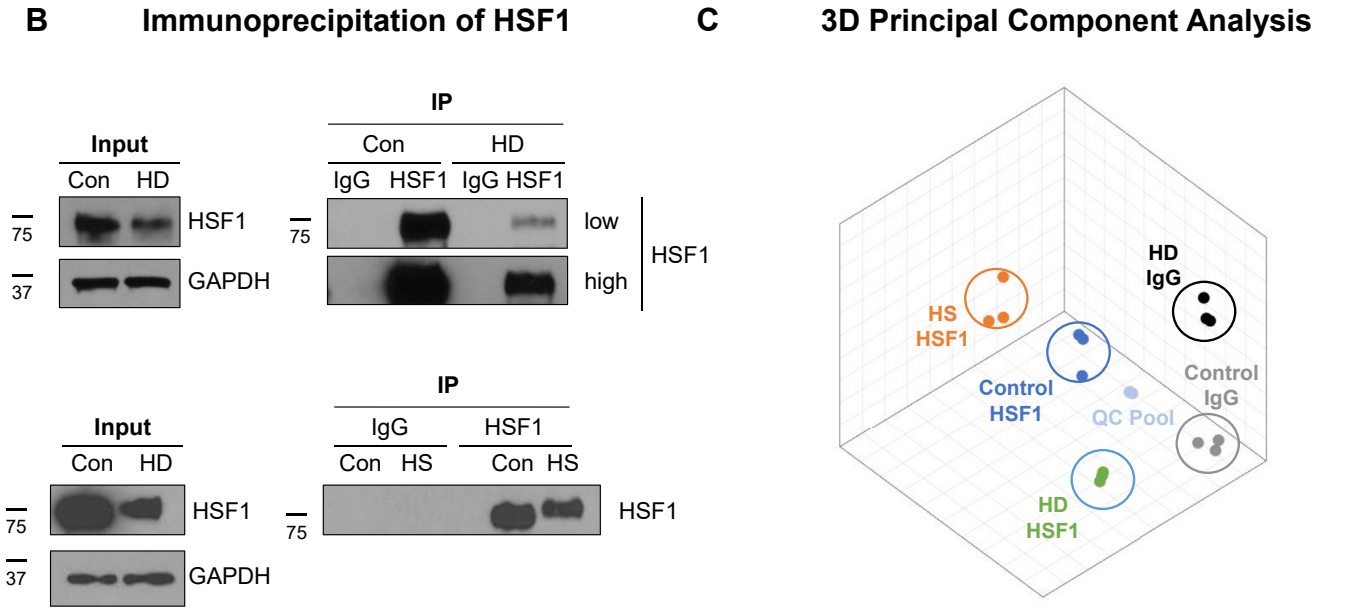

Figure 1. Outline of quantitative HSF1 protein interactome approach. *A*, endogenous HSF1 immunoprecipitation from biological triplicates using polyclonal anti-HSF1 antibody covalently liked to DynaG beads. HSF1-interacting proteins were identified by immunoblotting, silver-stained SDS-PAGE gels, and quantitative LC-MS/MS to compare the magnitude of interacting proteins across conditions analyzed. IgG was used as a negative control. *B*, immunoprecipitation of endogenous HSF1 in Control (Q7), Huntington's disease (HD, Q111), or heat shock (HS) as compared with negative control IgG. *C*, 3D Principal component analyses of the proteins identified in each sample demonstrate reproducibility of triplicates in the same biological context, whereas the separation of groupings in 3D space shows the differences in the HSF1 interaction network under the different evaluated conditions. Quality control (QC) pool is an equal mixture of the 15 independent biological samples tested and was used to assess technical variability across runs.

were identified in biological triplicate under the following conditions: unstressed Q7 cells (IgG immunoprecipitation [IP], HSF1 IP), Q7 cells after an acute heat shock (HSF1 IP), and HD cells (IgG IP, HSF1 IP), representing a total of 15 biological samples (5 experimental conditions × 3 biological replicas). Immunoprecipitation of HSF1 (Fig. 1, *A* and *B*, Fig. S1, *A* and *B*) demonstrates the enrichment of HSF1 and potential HSF1-interacting proteins as compared with IgG. In addition, a portion of the 15 biological samples were combined to create a QC pool used to account for any changes in the detection protocol throughout sample runs. Proteins were identified by LC-MS/MS, and runs were aligned based on the accurate mass and retention time of detected ions. In total, the initial dataset identified 12,497 unique peptides that were aligned to 1691 proteins. The coefficient of variation (% CV) for technical replicates of QC runs was 7.7%, and the biological variability was 20.9%, 29.5%, 24.2%, 18.6%, and 18.2% for the Q7 IgG, Q7 HSF1, Q7 HS HSF1, Q111 IgG, and Q111 HSF1 groups, respectively. The reproducibility of HSF1-interacting proteins identified from the three conditions was visualized with 3D principal component analysis (PCA) (Fig. 1*C*) and 2D PCA (Fig. S1*D*). Each PCA datapoint reflects the content and intensity of interacting proteins in the HSF1 or IgG IP-MS. Note that the clustering of biological replicates in 2D and

3D PCA indicates that highly similar protein components were identified in each replicate. In addition, separation of the different conditions in the PCA demonstrates the varied composition of the HSF1 interactome across conditions.

Validation of previously identified HSF1-interacting proteins

To eliminate low-confidence HSF1 interaction partners and proteins non-specifically immunoprecipitating, several restrictions were imposed on the identified proteins. First, hit proteins in the HSF1 IP must be enriched at least twofold over levels detected in the IgG IP and this difference must be statistically significant ($p < 0.05$) as determined by a t test calculated on $\log_2$-transformed intensity values. Lastly, to ensure proteins were correctly identified with sufficient peptide coverage, hit proteins were required to have a protein teller probability of 0.8 or higher. Protein teller probability determines protein identity based on all identified peptides, penalizing single-hit proteins and assigning common peptides to the simplest number of corresponding proteins (60). Excluding HSF1 itself, of the 1691 proteins identified, only 378 (22.4%) passed these stringent requirements; hit proteins in each condition are shown in blue (Control), orange (HS), and green (HD) (Fig. 2, *A–C*) and comprise the high confidence protein interaction partners of HSF1 for each condition evaluated in this study. Proteins in each condition that did not pass these criteria could still represent *bona fide* HSF1 interactions and are shown in gray.

Several previously reported HSF1-interacting proteins were detected, including BAG3 (49, 61, 62), X-ray repair cross complementing 5 (XRCC5, Ku80) (53), Pre-mRNA processing factor 8 (PRPF8) (50), rapamycin-insensitive companion of mTOR (RICTOR) (50), and structural maintenance of chromosomes protein 6 (SMC6) (Fig. 2*E* gray shading, underlined in Fig. 3 and Table S2) (63). Several HSF1-interaction partners closely functionally related to those previously described were also detected, including sorting nexin 9 (SNX9)—related to SNX4; importin subunit alpha-1 (IMA1, KPNA2)—related to KPNA3 and 4; and PAR12—related to PARP13 (HD only) (50, 54). Some of the discrepancies between the related proteins identified in this study may be attributed to differences in cell type, immunoprecipitation method, or specific stress conditions. Other identical or highly related HSF1-interacting proteins were strongly enriched in the HSF1 IP including CDC20 (64), HSPB1, and NDK7 (Fig. 2*E*) (61). However, owing to poor peptide coverage they were not above the stringent cutoff imposed for protein teller probability (Fig. 2*E*) (61).

HSF1 protein interaction networks span a wide variety of cellular functions

The interactome of HSF1 in this neuronal-like background comprises proteins of varied cellular function. Although some proteins interact with HSF1 across multiple cellular conditions, unique interactors were also found in each condition (Table S2). The number of shared and unique HSF1-interacting proteins in control, heat shock, and HD conditions are shown in Figures 2*D* and S2, *A–C*. In general, fewer HSF1 protein interactions (10 unique) were detected that met our criteria in control conditions compared with HS (106 unique) and HD (119 unique); HD and HS shared a considerable (48%–52%) overlap, suggesting that some of these interactions may be stress dependent or common for HSF1 activation. However, HS and HD conditions also maintained many unique protein interactions, underscoring the potential differences in protein regulation exerted on HSF1 during the acute temperature stress and chronic stress of protein misfolding. In response to heat shock, HSF1 interacts with many proteins involved in nuclear import and degradation; 8% of heat shock–specific HSF1 interactions involve nuclear import machinery such as importins (α, β, 4, 5, 7, and 9) and nuclear pore proteins (Nup93), whereas 33% involve degradation, such as ubiquitin ligases (Nedd4, TRI56) and proteasomal subunits and proteases (PSA1–7, PSD11–13) (Table S1). These HS-specific interactions suggest that transient HSF1 activation involves the nuclear import machinery, interaction with RNA Pol II subunits (RPB1-3), and degradation machinery. Although these interactions are not observed in chronic stress, HSF1 does interact with many proteins specifically in HD cells (Table S2). For instance, HD-specific interactions are enriched for RNA processing factors, including many members of the DEAD-box helicase families and the RNA exosome complex. In addition, several proteins involved in DNA repair interact with HSF1 specifically in HD, including XRCC5, SMC5-6, and PARP12.

To further explore how the constellation of HSF1-interacting proteins are changed between control, heat shock, and HD conditions, the intensity of the interactions shared between two or more conditions was assessed (Fig. 3). When comparing the magnitude of HSF1-interactors, only proteins with abundance that were greater than threefold different between conditions ($p < 0.05$) were considered as high-confidence changes. With these criteria, most of the proteins interacted with HSF1 to a similar extent when comparing control and stress conditions; 78% of the shared interactions between control and HS and 92% of control and HD were preserved to a similar magnitude (gray boxes, Fig. 3). In contrast, only ∼52% of the shared interactions in HS and HD were unchanged. Interestingly, for shared interactions that were different between HS and HD conditions, all HSF1-interacting proteins interacted to a larger extent under HS conditions than in HD cells (red boxes, Fig. 3).

Overall, HSF1 interacts with proteins of broad cellular function including those involved in chromatin remodeling, protein trafficking, protein QC, and translation and transcriptional coactivators and repressors (Fig. 4). Of particular interest are the many chromatin remodeling proteins detected. Although this study does not differentiate between direct HSF1 interactions and those that operate as a complex containing other proteins, previous studies have demonstrated the importance of recruitment of chromatin remodelers, such as BRG1 of the SWI/SNF multiprotein chromatin remodeling complex, for HSF1-driven transcription (51, 65). Some of the chromatin remodeling proteins identified in this study include histone demethylase NO66 and RuvBl1 and RuvBl2 helicases, components of the NuA4 histone acetyltransferase complex

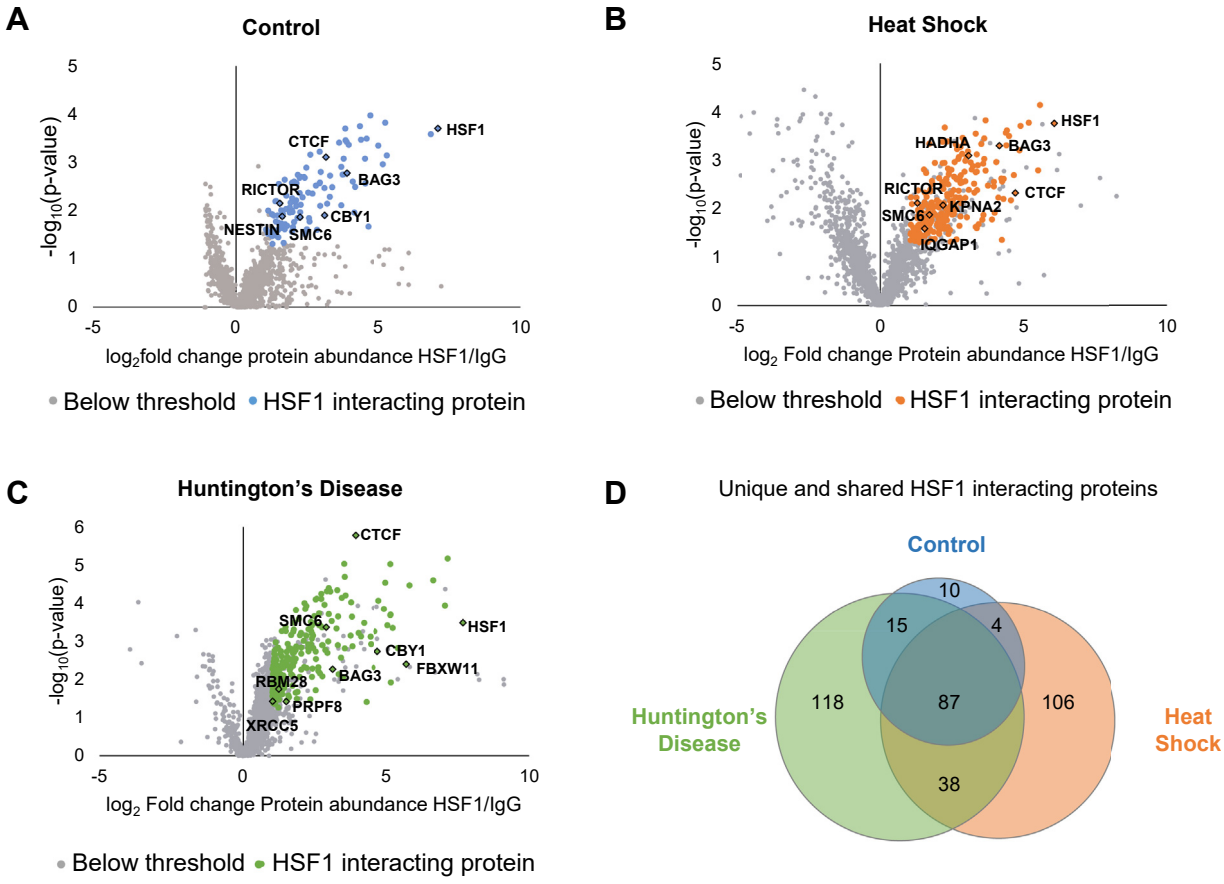

E

Reported HSF1-interacting Protein	Identical protein in this study	Condition detected
PRPF8[50]	PRP8	HD
SNRNP200[50]	U520	HD
RBM28[50]	RBM28	HD
IQGAP1[50]	IQGA1	HS
RICTOR[50]	RICTR	Con, HS, HD
NESTIN[50]	NEST	Con
HADHA[50]	ECHA	HS
XRCC5 (Ku80)[53]	XRCC5	HD
BAG3[61,62]	BAG3	Con, HS, HD
SMC5[105]	SMC5	HD
SMC6[63,105]	SMC6	Con, HS, HD
NEDD4[59]	NEDD4	HS
CBY1[63]	CBY1	Con, HS, HD
Nme7[61]	NDK7	*poor peptide coverage*
CDC20[64]	CDC20	*poor peptide coverage*
HspB1[61]	HSPB1	*poor peptide coverage*
CCDC88A[50]	DAPLE (CCDC88C)	*poor peptide coverage*
Reported HSF1 interacting Protein	**Related protein in this study**	**Condition detected**
SNX4[50]	SNX9	HS
KPNA1, KPNA3[50]	IMA1 (KPNA2)	HS
PARP1, PARP13[54]	PAR12 (PARP12)	HD
FBXW7[33]	FBW1B (FBXW11)	Con, HS, HD
SMARCA4 (BRG1)[50,65,95]	SMCA5 (SMARCA5)	Below fold change threshold

Figure 2. Protein-interactors identified in control, heat shock, and Huntington's disease cell models with HSF1 immunoprecipitation–mass spectrometry. *A–C*, volcano plot of HSF1-interacting proteins in Control *A*, HS *B*, and HD *C*; proteins passing fold change >2, $p < 0.05$, and Protein-Teller probability >0.8 are highlighted in blue, orange, and green, respectively. Proteins below these thresholds are shown in gray. Several previously reported HSF1-interacting proteins and select proteins of interest are highlighted with text. *D*, Venn diagram showing the shared and distinct interactions of HSF1 observed in each condition. *E*, some of the proteins identified in this study that are identical to (*dark gray*) or highly similar to (*light gray*) previously reported HSF1-interacting proteins, with references to previous reports (33, 50, 53, 54, 59, 61–65, 95, 105).

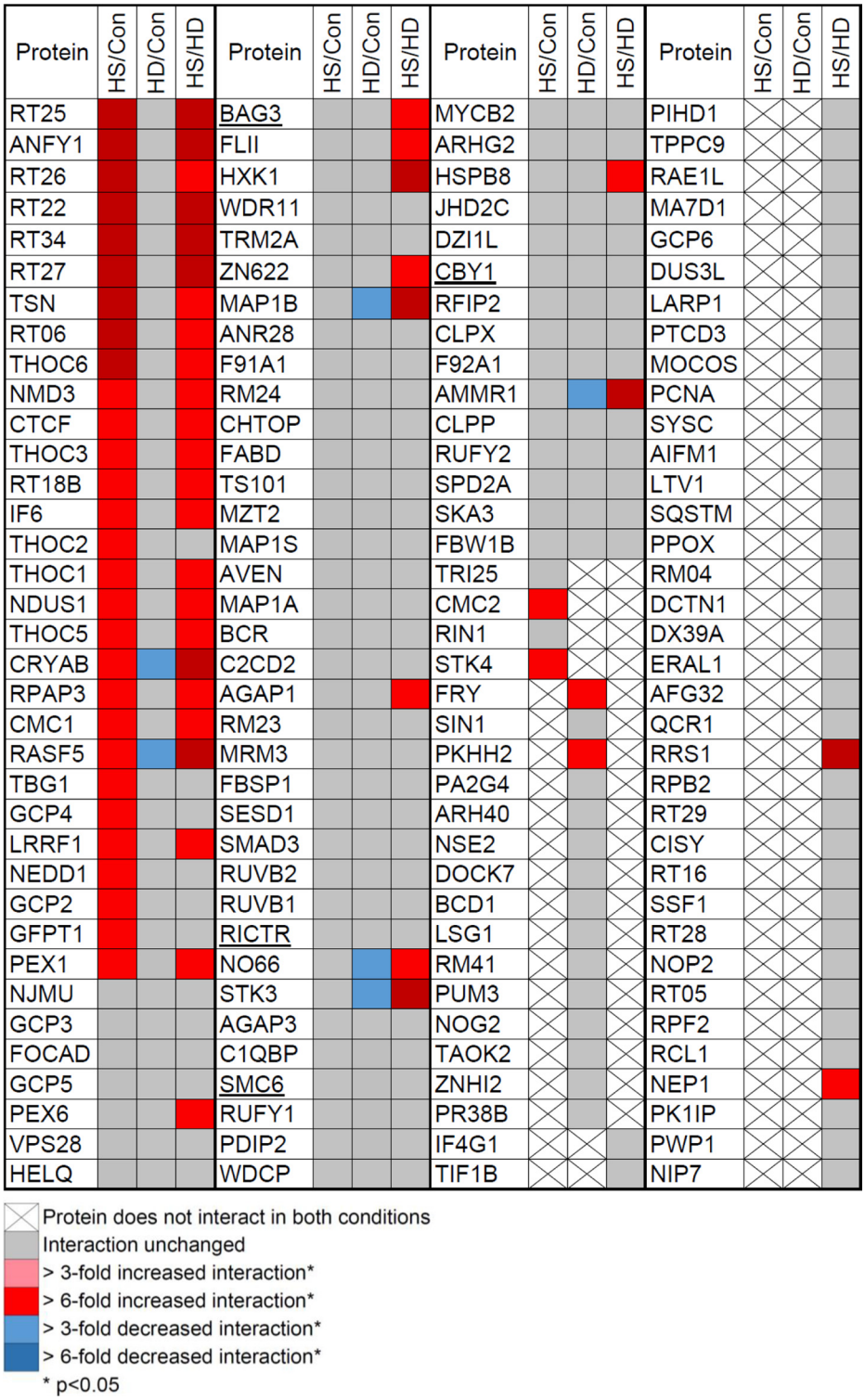

Figure 3. Heat map of HSF1-interacting proteins shared in two or more conditions. The magnitude of the interacting protein detected in each condition was compared; magnitude of interaction was calculated from robust mean normalization of raw intensity values for each protein present in the HSF1 IP (see Table S1). Interactions that changed by threefold (down, *light blue*; up, *light red*) or sixfold (up, *dark red*; down, *dark blue*) with statistical significance ($p < 0.05$) are indicated. Proteins found in similar levels across conditions are colored *gray*. Proteins indicated with crosses were not found in both indicated conditions and were not compared. Underlined proteins indicate those recapitulated from previous studies (see Fig. 2*E*).

involved in transcriptional activation. RuvBl1/2 interact with and regulate the activity of other DNA-binding proteins, such as Myc and β-catenin (66). Lastly, many different proposed transcriptional activators, such as JHD2C and canonical repressors, were found to interact with HSF1, including NFX1 and CTCF. These proteins may provide mechanistic insight into how HSF1 mediates gene repression, a largely unexplored aspect of HSF1 biology that contributes to disease conditions

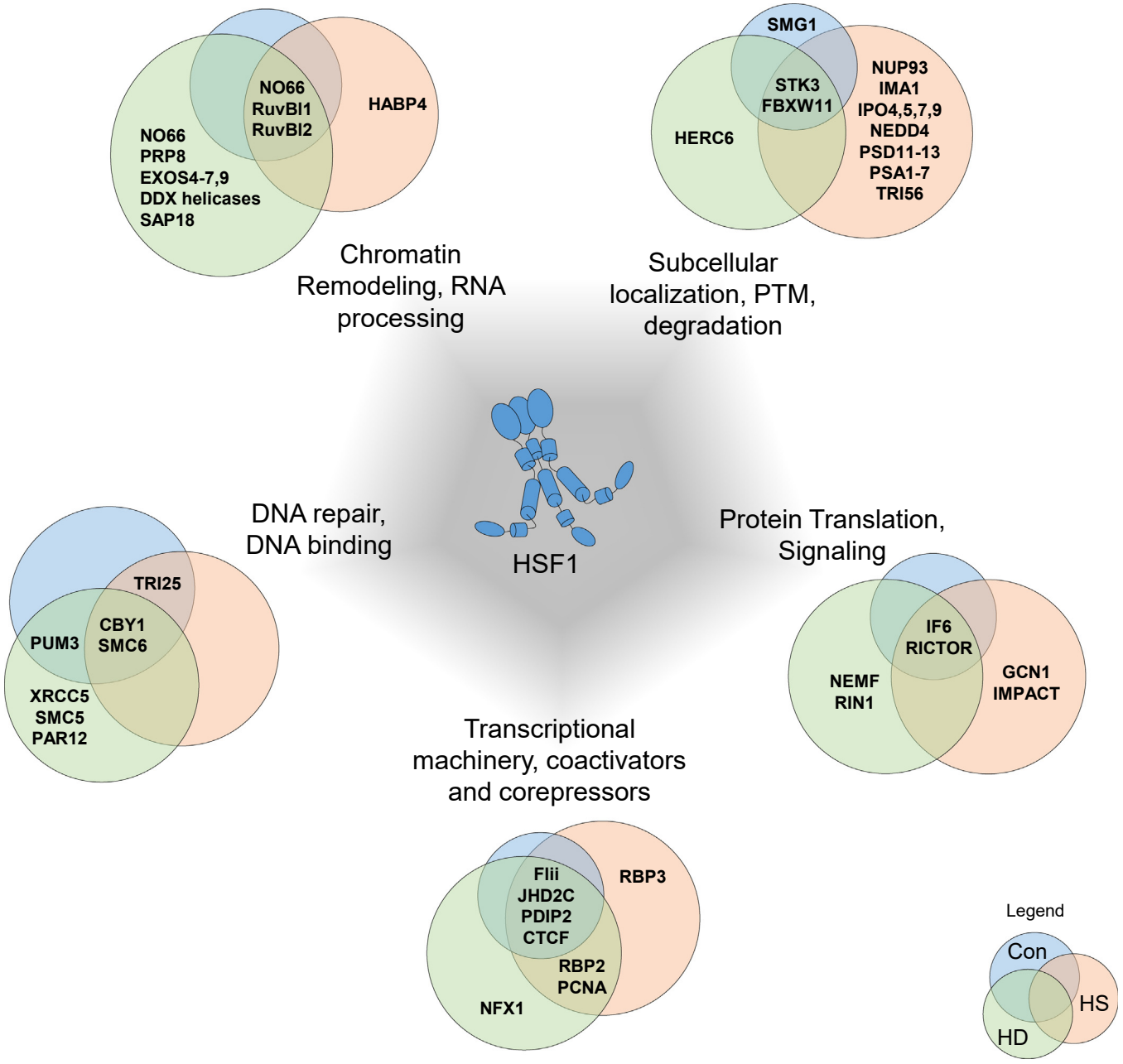

Figure 4. HSF1 Interactome in the different stress conditions, showing. HSF1-interacting proteins from select functional categories in unstressed (Con, *blue*), heat shock (HS, *orange*), and Huntington's disease (HD, *green*).

through a network of HSF1-repressed genes in cancer (19) and other gene targets involved in inflammation (20–22, 52).

HSF1 is well known for its role in stress-regulated gene activation, but it also serves to repress gene expression (19–22, 52). Because of its role as a multi-functional transcriptional regulator, one HSF1-interacting protein of particular interest is CCCTC-binding factor (CTCF), a high-confidence interactor in unstressed, heat shocked, and HD cells (Fig. 2, *A*–*C*). CTCF is a transcriptional regulator that binds DNA and proteins, including other transcription factors, via eleven zinc fingers, to coordinate transcriptional regulation across many loci throughout the genome (67). CTCF also participates in chromatin organization, gene insulation, gene activation, and gene repression by promoting interactions of chromosomal DNA and recruiting chromatin remodeling enzymes (67–69). CTCF interacts with several other DNA-binding proteins, including Y-box–binding protein, multifunctional transcription factor YY1, and Kaiso, and regulates their function (67). In addition, a previous HSF1 chromatin immunoprecipitation (ChIP)-seq study revealed high co-occupancy of CTCF at HSF1-bound sites (26). Based on the HSF1–CTCF co-occupancy at regions with histone 4 acetylation, but lacking RNA polymerase II, it was proposed that CTCF may play a role at untranscribed regulatory elements during heat stress (26). Interestingly, CTCF also showed high co-occupancy with HSF1 at other categories of HSF1-bound loci, including promoters of HSF1

target genes (26). Because of the HSF1–CTCF interaction identified in this study, and the previous observation that CTCF and HSF1 bind at highly overlapping loci (26), we explored the functional consequences of the CTCF–HSF1 interaction.

A direct interaction between HSF1 and CTCF is stimulated by acute stress

To independently validate the quantitative CTCF–HSF1 interaction observed from HSF1 IP-MS (Fig. 5*A*), endogenous HSF1 was immunoprecipitated from HEK 293T cells transfected with hemagglutinin-tagged CTCF (HA-CTCF) and HA-CTCF was probed by immunoblotting. HSF1 robustly interacted with CTCF in unstressed cells but did not interact with the negative control IgG precipitate (Fig. 5*B*). In addition, the increased HSF1–CTCF interaction observed in heat-stressed cells by IP-MS (Fig. 5*A*) was recapitulated by pull-down of HA-CTCF in control and heat shock–treated HEK 293T cells, with which HSF1 co-purified to a greater magnitude in heat shock conditions (Fig. 5*C*).

HSF1 harbors multiple domains of distinct function. To determine which region of HSF1 interacts with CTCF, plasmids encoding FLAG-tagged HSF1 truncations were constructed (Fig. 5*D*) and expressed by transfection into 293T stable HSF1-knockdown cells (Fig. S3*A*) to prevent hetero-multimerization with endogenous HSF1. CTCF co-purified only with HSF1 truncations containing the DBD, whereas HSF1 ΔN1, lacking the DBD, failed to interact with CTCF (Fig. 5*E*). To evaluate whether the interaction with CTCF requires HSF1 that is competent for DNA binding, the critical Arg residue (R) of the HSF1 "SFVRQ" DNA binding recognition helix was mutated to Ala (HSF1 R71A). This Arg residue is necessary for HSF1 DNA binding competence and makes sequence-specific contacts to the guanine of the nGAAn heat shock element (HSE) sequence, to which HSF1 binds (70–73). In stable HSF1 knockdown HEK 293T cells, both wildtype HSF1 and HSF1 R71A interacted with CTCF under control and heat shock conditions (Fig. 5*F*). Similar results were obtained by comparing HA-CTCF co-purification with WT and R71A HSF1 in HSF1$^{-/-}$ mouse embryonic fibroblasts (Fig. S3*B*). These results indicate that the DNA binding activity of HSF1 is not required for interaction with CTCF.

To determine if the HSF1–CTCF interaction requires additional proteins *in vivo*, an *in vitro* pull-down using purified components was conducted. Human, codon optimized STREP-HSF1 and CTCF-His were expressed in *Escherichia coli* and purified by affinity chromatography (Fig. 5*E*). In an *in vitro* STREP pull-down, we observed co-purification of CTCF in the presence of STREP-HSF1, but not in the absence of HSF1 (Fig. 5*H*). This indicates that CTCF and HSF1 interact directly *in vitro* in the absence of other mammalian proteins.

CTCF and HSF1 show overlapping profiles of potential repression targets

Although several studies have explored stress-induced gene transcription by HSF1, fewer have focused on how HSF1 exerts control over basal transcription and what regulatory factors may affect this. As CTCF may likely exert its regulatory function at the level of chromatin architecture and the three-dimensional chromatin structure is largely conserved in response to heat shock (74), this study focuses on HSF1 and CTCF in the unstressed state. To begin to understand how CTCF may influence basal HSF1-mediated transcription, transcript abundance was analyzed by RNA-seq in HEK 293T cells during transient siRNA-mediated knockdown of CTCF or HSF1. This study explored transcriptional changes during normal growth conditions, during which the CTCF–HSF1 interaction is observed (Fig. 5). Four biological replicates of each condition were collected and demonstrated strong correlation of transcriptional profiles with Spearman coefficients greater than 0.95 (Fig. S4*A*). CTCF and HSF1 knockdowns successfully and robustly depleted target transcripts (14% and 23% of HSF1 and CTCF mRNA abundance, respectively, were observed compared to with negative control siScr) and do not impact partner protein, transcript abundance, or splicing (Fig. 6*A*, Fig. S4, *B* and *C*). Transcriptional changes of siRNA-targeted and negative control samples were assessed with DESeq2, categorizing genes as significantly changed as either high or low confidence ($p < 0.001$), unregulated, or unexpressed. Genes with a minimum fold change of 1.25 were considered high confidence calls and are reported here as up- or down-regulated. Under these conditions, 501 down-regulated transcripts were observed upon HSF1 depletion; these could be basal targets for HSF1 activation, although many are likely regulated in a non–HSF1-dependent manner (Fig. 6*B*). Similarly, 316 transcripts were found with higher abundance in siHSF1-treated cells, some of which may be HSF1 repression targets (Fig. 6*B*).

Changes in a battery of established CTCF and HSF1 gene targets demonstrate that knockdown in these conditions resulted in predicted changes in target gene expression. Transcript levels of established HSF1 targets were altered, including both activation and repression targets. For example, the abundance of HSF1 activation targets DNAJA1, HSPA1B, HSPA14, JMJD6, and CKS2 was reduced in siHSF1 treatment (Fig. 6*C*). HSF1 repression targets PBLD and CELSR1 were de-repressed in siHSF1-treated cells (Fig. 6*C*). Expression of the MMAA and FCGBP genes, established CTCF repression targets, is de-repressed in siCTCF-treated cells (69) (Fig. 6*C*). On the other hand, activation targets of CTCF such as RAG1 and FAM131C showed lower mRNA abundance in siCTCF-treated cells (Fig. 6*C*). Comparison of the up- and down-regulated genes in siHSF1 or siCTCF cells revealed a strong overlap, particularly for genes with potential HSF1 repression. Although 94 of the 501 down-regulated genes in siHSF1-treated cells were shared with siCTCF-treated cells, 124 of the 316 up-regulated genes in siHSF1 cells were up-regulated also in the absence of CTCF (Fig. 6*D*). To assess if the individual genes shared in siHSF1 and siCTCF treatments were changed to a similar magnitude, the transcriptional changes of potential activation and repression targets were compared. The Pearson correlation of potential repression targets was higher than all detected transcripts (Fig. S4*D*) and more

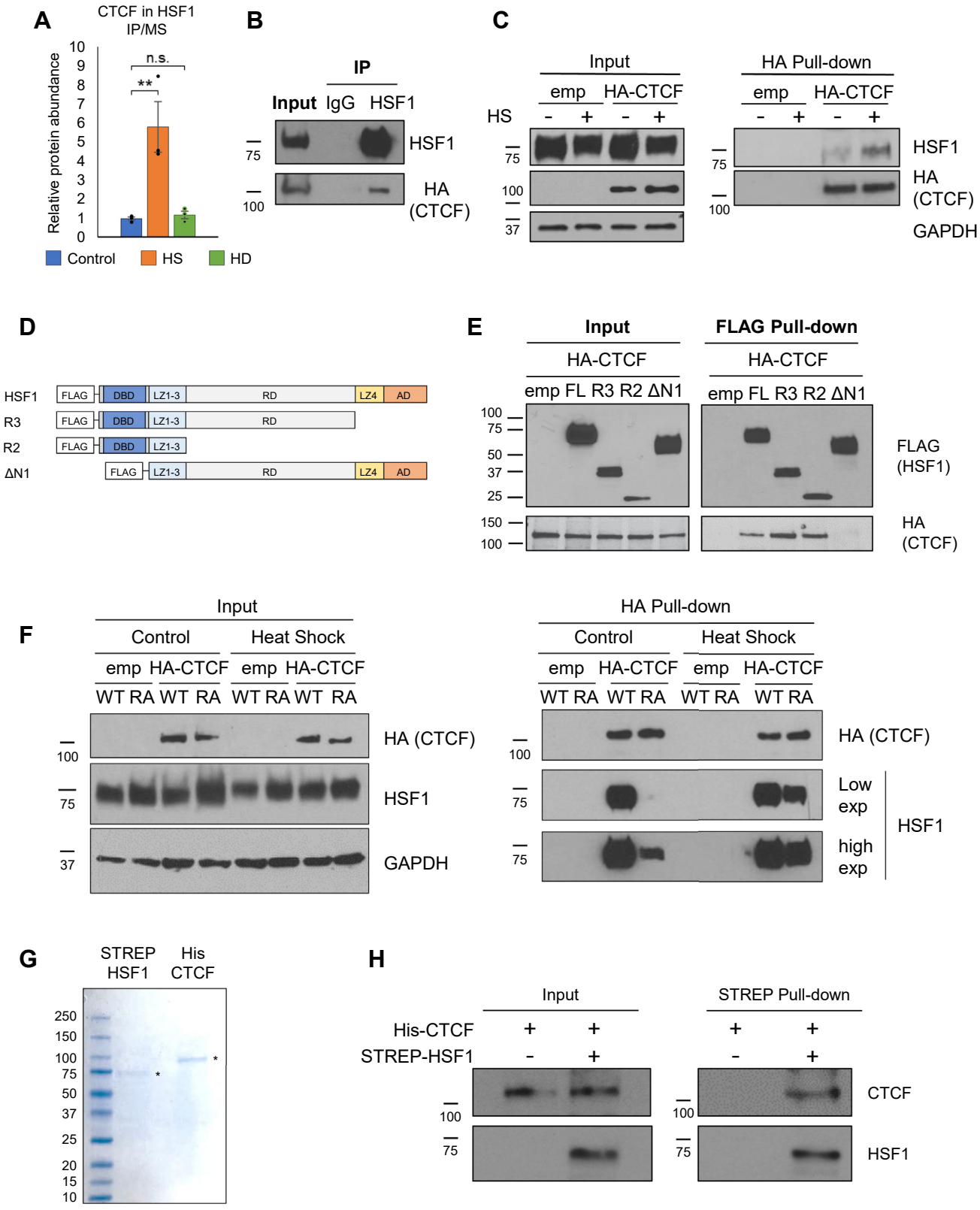

Figure 5. HSF1 interacts with CTCF via the DBD but does not require HSF1 DNA binding. *A*, HSF1 IP-MS analysis demonstrated increased CTCF levels in the HSF1 IP; individual datapoints for biological replicates are shown as *black dots*, whereas the bars in each condition indicate the average protein abundance relative to control conditions. *B*, endogenous HSF1 or IgG control immunoprecipitation from HEK 293T cells transfected with a plasmid expressing HA-CTCF. *C*, HA pull-down from HEK 293T cells transfected with HA-CTCF in control or heat shock (30 min, 42 °C) conditions. *D*, diagram of FLAG-tagged HSF1 truncations used in *E* with the FLAG epitope tag and HSF1 domains indicated. *E*, stable HSF1-knockdown cells transfected with a plasmid expressing HA-CTCF and either empty vector or FLAG-HSF1 wildtype or the indicated truncated proteins; the FLAG-HSF1 pull-down was conducted and followed by immunoblotting with anti-HA (CTCF) antibody. *F*, stable HSF1-knockdown cells transfected with empty vector or plasmids expressing HA-CTCF

correlated than potential activation targets, showing a Pearson correlation of 0.820 versus 0.381 (Fig. 6*E*). The strongly correlating changes in mRNA levels in siHSF1 and siCTCF cells likely reflects the importance of CTCF in preparing chromatin architecture for transcriptional regulation. In addition, the physical interaction of HSF1 and CTCF under non-stress and stress conditions demonstrates the importance of controlling HSF1 and its interactome in both physiological and pathophysiological conditions.

Discussion

The regulation of HSF1 in response to acute stress has been studied since the discovery of the heat shock response in the early 1960s (75). More recently, the dysregulation of HSF1 and the crucial roles this stress-protective transcription factor plays in the pathophysiological contexts of both neurodegenerative disease and cancer have been of great interest (18, 19, 33). Studies have shown the diminution in HSF1 levels in neurodegenerative diseases including HD, Alzheimer's disease, and Parkinson's disease and the dysregulation of HSF1 target gene expression (33, 59, 76–78). In HD, HSF1 genome-wide binding and transcriptional network regulated by HSF1 are disrupted and impaired HSF1 function further exacerbates chronic protein misfolding (28, 33, 79). In contrast, in cancer, high levels of active, nuclear HSF1 support malignancy by coordinating a transcriptional signature partially distinct from heat shock, including targets that regulate cell cycle progression, chaperone production, and repression of apoptotic factors (19). A more thorough understanding of the regulation of HSF1 could offer new insights into how HSF1 is altered in different disease states. Because one major mechanism for HSF1 regulation is driven by protein–protein interactions (22, 24, 50, 51, 54), this study explores how the networks of HSF1-interacting proteins are altered in control conditions and those of heat shock and chronic protein misfolding such as that observed in HD. In addition, in contrast to previous HSF1-proteomics studies, this study utilized mouse cells derived from the striatum of the brain, the area most affected in HD, and therefore may reflect regulatory interactions specific to cells in the central nervous system in a normal context and in disease.

This study found a highly diverse group of HSF1-interacting proteins with broad cellular functions. Overall, HSF1 interacts with more proteins in response to acute or chronic stress compared with basal conditions, where many of these stress-induced interactions are shared between heat shock and HD but are of lower magnitude in HD. One such protein is serine threonine kinase (STK3), which is activated by pro-apoptotic stimuli; STK3 showed an ∼ sixfold reduced interaction in HD compared with control cells and interacted with HSF1 ∼ tenfold more in acute heat shock than HD; HSF1 is known to be regulated by various post-translational modifications, including phosphorylation events, and the role of STK3 in modulating HSF1 is currently unexplored. In addition, chibby family member 1 (CBY1) was identified in our study in all conditions tested and in a previous unbiased, multi-protein interactome study (63); CBY1 is known to interact with and regulate several other proteins, including β-catenin and thyroid cancer-1 (TC-1) (80). Further investigation of HD-specific interactions may reveal new ways that HSF1 regulation is altered in chronic protein misfolding stress. Interestingly, HSF1 in HD was found to interact with several proteins involved in DNA repair including SMC5 and SMC6, XRCC5, and PARP12. DNA repair pathways have been implicated in the advancement and onset of HD and other trinucleotide repeat diseases as they can contribute to the further expansion of the disease-causing trinucleotide tract (81, 82). Investigation of these protein interactions may reveal a role for HSF1 in genome integrity in HD as previously shown for mammary tumors (54). Another protein of interest identified in HD conditions in this study is nuclear export mediator factor (NEMF), a component of the ribosome QC complex. In yeast, translational stress activates HSF1 in a manner distinct from heat shock, and the highly conserved yeast homolog of NEMF, Tae2, is critical for the transmission of translational stress to yeast HSF (83). Data described here suggest that the HSF1–NEMF interaction, and the potential role this interaction serves in the RQC-stress response pathway, may be conserved in higher eukaryotes. In addition, the possible functional consequence of the interaction of HSF1 with pre-mRNA processing factors observed by us (PRP8, PRP17), and PRP8 by others (50), has yet to be explored.

Although many chaperone proteins including Hsp70, Hsp90, and subunits of the TRiC–CCT complex were detected in the HSF1 immunoprecipitation, most were not sufficiently enriched in the HSF1 IP over the negative control IgG IP to meet our strict threshold. This may, in part, be due to the low affinity of the HSF1-chaperone interactions described. For instance, a recent study found that HSF1 only interacts with a subset of Hsp90 conformations and thus the overall affinity of HSF1 for endogenous HSP90, which is sampling many different conformations, is relatively weak (84). A similarly low-affinity interaction of yeast HSF1 with the CE2 region of Hsp70 was biochemically characterized (10). Furthermore, multiple Hsp70-binding sites have different affinities for human HSF1, the interaction of which functions to unwind HSF1 oligomers (85). Lastly, the profound technical differences in HSF1 IP-MS techniques used in this study as compared with those studies optimized for the identification of chaperone interacting proteins (86) could certainly contribute to the relatively small number of HSF1-interacting chaperone proteins identified in this study.

It is currently unclear why and how HSF1 interacts with more proteins in response to stress, but this could be a function of its oligomerization, nuclear localization, or

and WT HSF1 or R71A HSF1, harboring a mutation that abrogates HSF1 DNA binding, followed by HA pull-down and immunoblotting with anti-HSF1 antibody. *G*, Coomassie-stained SDS-PAGE gel of purified STREP-HSF1 and His-CTCF used in *H. H, in vitro* STREP purification of His-CTCF alone or together with STREP-HSF1, followed by immunoblotting with anti-CTCF and anti-HSF1 antibodies.

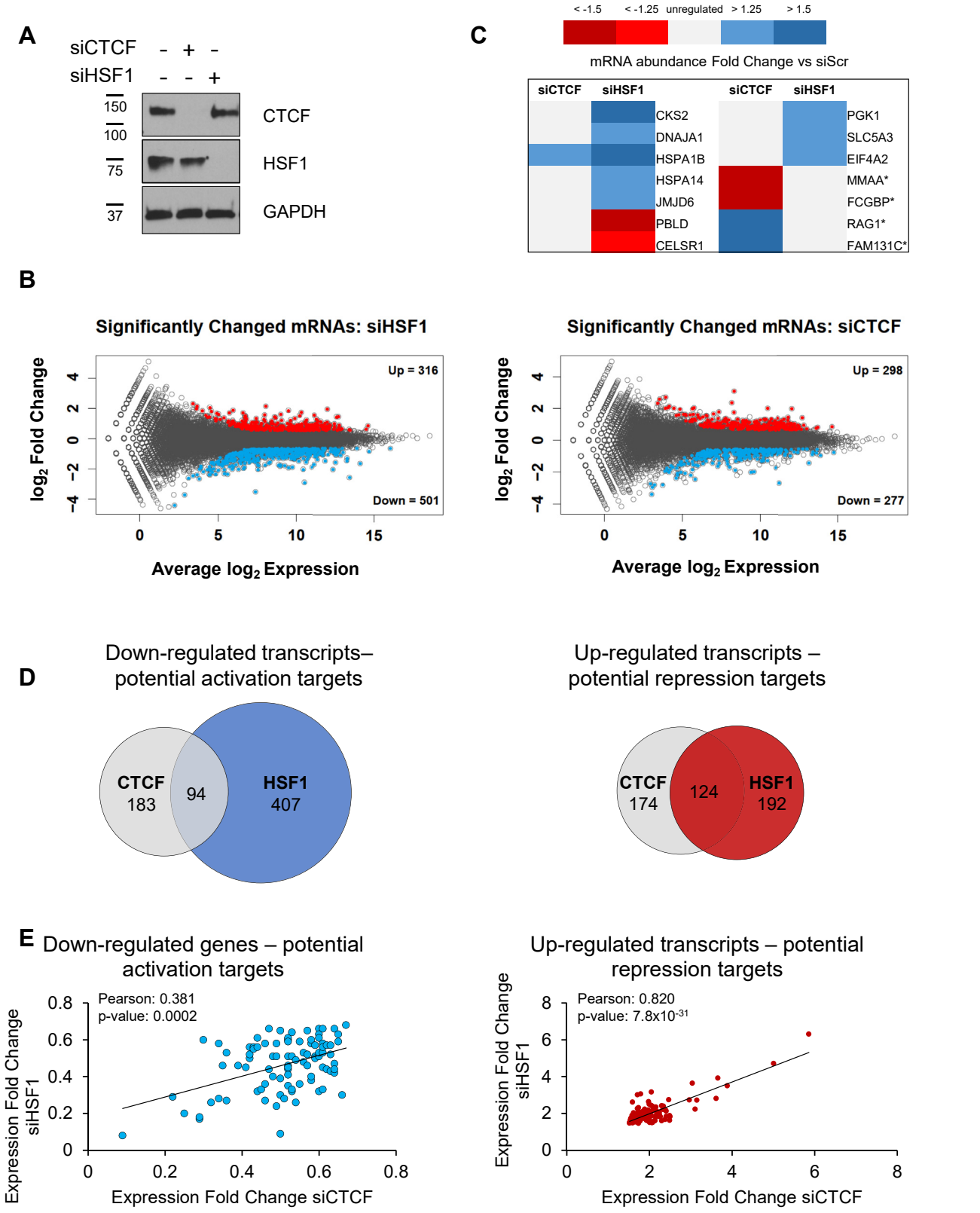

Figure 6. Role of CTCF in HSF1-mediated basal transcription. *A*, protein extracts generated from HEK 293T cells transfected for 48 h with siRNA targeting HSF1, CTCF, or scrambled control. *B*, DESeq2 analysis revealed significant ($p < 0.001$) high confidence changes in transcript abundance in the HSF1 or CTCF siRNA treated cells. *C*, transcript abundance of previous established HSF1 (19, 106) or CTCF targets (69) (* indicates CTCF target genes) as assessed by RNA sequencing (n = 4). *D*, overlap of down- and up-regulated genes for siHSF1 or siCTCF treated cells; numbers indicate the quantity of distinct transcripts in each category. *E*, Pearson correlation of down- and up-regulated genes for siHSF1- and siCTCF-treated cells.

stress-induced post-translational modifications that drive specific regulatory interactions. For example, in the case of CTCF, a nuclear protein, the retention of HSF1 in the nucleus and increased level of chromatin-bound HSF1 would explain the increased interaction in response to acute heat stress as compared with unstressed cells. Whether these other, unexplored HSF1 interactors alter HSF1 function remains to be determined. What is clear is the distinct HSF1-interacting networks in unstressed, heat shock, or HD cells; future studies of these protein interactors may reveal new facets of HSF1 biology or new HSF1 regulatory mechanisms. In particular, determining if any of the observed interactions are striatum specific may provide insight into how HSF1 is regulated in the striatum, the area of the brain that is most affected in HD (35).

One highly interesting HSF1-interacting protein observed was CTCF, which is primarily known for its role in chromatin organization and transcriptional repression (68, 87). CTCF and HSF1 interact *in vivo* and directly *in vitro*, and the potential repression targets of CTCF and HSF1 overlap more strongly than activation targets. A previous study found a high occupancy of CTCF at HSF1-bound, particularly at untranscribed regions (26). A more recent study found that, among known and other proposed coregulators, CTCF is detected at HSE-bound HSF1 but not at mutated HSEs (88). Based on these innovative studies, the direct protein interaction observed in our study, and the strong correlation of upregulated genes in HSF1 or CTCF knockdown, we suggest that CTCF may be important for targeting HSF1 to the CTCF-rich regions in the chromatin and in HSF1-mediated gene repression.

CTCF could affect HSF1-mediated transcription in several ways, including establishing and altering chromatin looping interactions between transcription regulatory elements such as promoters, enhancers, and insulators. Altered chromatin interaction probabilities could, in turn, affect RNA Pol II regulation at connected distal regions likely via other mechanisms. It remains to be determined whether CTCF can recruit HSF1 to CTCF-primed regions accessible for transcription factor binding, or by HSF1 recruiting CTCF at HSE-bound sites (26, 67, 88–91). CTCF can mediate a versatility of changes in chromatin architecture by preventing the encroachment of heterochromatin and by recruiting chromatin remodeling proteins, including enzymes catalyzing histone acetylation or methylation (67, 68, 92, 93). Like many transcription factors, HSF1–DNA binding depends on the chromatin architecture; in some cases, protein interaction partners of HSF1 influence these chromatin changes (25, 94). HSF1 interacts with replication protein A, and this complex recruits histone chaperone FACT, resulting in opening of the chromatin structure (50). In addition, the transcriptional activation domain of HSF1 interacts with BRG1, a SWI/SNF chromatin remodeling complex, and this is important for the production of full-length Hsp70 (65, 95).

Although this study does not encompass how CTCF may affect genome-wide binding of HSF1, it raises questions of the purpose of the HSF1–CTCF interaction. Whether CTCF is involved in facilitating HSF1 DNA binding through protein-protein interactions, or via chromatin remodeling, remains to be determined. Interestingly, CTCF has been implicated in regulation of DNA binding of other proteins, including TAF3 (96), which was previously shown to be necessary for chromatin architecture and HSF binding in *Drosophila* cells (97). Future studies will determine whether CTCF modulates HSF1 target gene transcription, but our data suggest that the involvement of CTCF may be, in part, for HSF1 basal repression targets. Future studies may also address how HSF1 stress-induced transcription is affected by CTCF and what other factors affect this protein–protein interaction, like post-translational modifications. The repressive function of HSF1 has become increasingly important in recent light of the targets repressed by HSF1 that contribute to disease, including inflammation, apoptosis, and protein misfolding diseases, such as Tau (19–22, 52, 98–100).

Experimental Procedures

Cell culture and cell lines

Cell lines used in this study were as follows: mouse-derived striatal cells STHdh(Q7) and STHdh(Q111) (Coriell Cell Repositories), 293T human embryonic kidney (HEK) cells (ATCC CRL-1573), stable shScr and shHSF1 HEK 293T cells (generated in this study), and $HSF1^{-/-}$ mouse embryonic fibroblast (MEF) cells (from Dr Ivor Benjamin, Medical College of Wisconsin). Striatal cells were maintained at 33 °C in Dulbecco's modified Eagle's medium (DMEM) supplemented with 10% fetal bovine serum (FBS) and 91 μg mL^{-1} Normocin (InvivoGen). HEK 293T cells were grown at 37 °C in DMEM supplemented with 10% FBS and 91 μg mL^{-1} Normocin. $HSF1^{-/-}$ MEF cells were grown at 37 °C in DMEM supplemented with 10% FBS, 0.1 mM nonessential amino acids, 100 U ml^{-1} penicillin/streptomycin, and 55 μM β-mercaptoethanol. Striatal cells (STHdhQ7 and STHdhQ111) were authenticated by immunoblotting with mHtt–specific antibody (MAB2166) (33). The $HSF1^{-/-}$ MEF cells were authenticated by immunoblotting for HSF1 with multiple anti-HSF1 antibodies (Enzo 10H8, and Bethyl [5]).

Heat shock

Cells treated with heat shock were incubated at 42 °C for 30 min and compared with cells grown at normal growth temperatures (33 °C for StHdh cells, 37 °C for 293T and MEF cells).

Endogenous HSF1 immunoprecipitation

For HSF1 IP-MS analysis, endogenous HSF1 was immunoprecipitated from cells lysed in IP buffer (20 mM HEPES, 5 mM $MgCl_2$, 1 mM EDTA, 100 mM KCl, 0.03% NP-40, 1% Triton X-100) supplemented with 1X HALT protease and phosphatase inhibitor cocktails (ThermoFisher). Protein lysates were cleared with centrifugation (14,000 r.c.f., 4 °C, 15 min), and protein concentrations were quantified with bicinchoninic acid assay method (Pierce). Samples were normalized to 1 mg ml^{-1} and precleared with DynaG beads for 3 h. DynaG magnetic beads covalently cross-linked to either

negative control IgG (Bethyl) or HSF1 (Bethyl) (5) were added to samples and incubated overnight at 4 °C rotating. Beads were washed four times with IP buffer and eluted with 50 µl of TES (10 mM Tris pH 7.5, 1 mM EDTA, 0.5% (w/v) SDS) at 65 °C, 10 min. Eluates were snap frozen in liquid nitrogen until being processed by mass spectrometry, immunoblot, or silver-stained gel analysis. For HSF1 immunoprecipitation not used for mass spectrometry, the protocol above was identical except DynaG beads were not covalently linked to antibodies. Instead, antibodies were incubated with lysates overnight, and subsequently, beads were added and incubated for 3 h before the washes and elution. HA and FLAG pull-downs were performed in the same manner using anti-HA magnetic beads (Thermo Scientific) or anti-FLAG M2 magnetic beads (Sigma). HA pull-downs were eluted in 0.1 M glycine pH 2.0, and samples were neutralized using 1M Tris pH 8.5 or TES; FLAG pull-downs were eluted in TES.

Covalent linkage of antibody to beads

To couple the beads and antibody, DynaG beads were incubated with IgG or HSF1 in phosphate buffered saline (PBS) for 3 h at 4 °C (30 µl beads per 20 µg antibody, 1 ml PBS). Antibody-coupled beads were washed three times with 0.2 M sodium borate pH 9.0 and cross-linked with freshly made 20 mM dimethylpimelimidate dissolved in 0.2 mM sodium borate pH 9.0. Cross-linking was performed for 40 min at room temperature with rocking, followed by three washes with acid wash buffer (0.58% v/v acetic acid, 150 mM NaCl) and three washes with ice cold PBS. Beads were prepared and used the same day for subsequent immunoprecipitation experiments.

Mass spectrometry

Samples were diluted in TES and 1X Laemmli/SDS buffer, which were supplemented with 1 µl 200 mM DTT each, and heated at 70 °C for 10 min. Forty-nine microliters of each sample was loaded onto an Invitrogen NuPAGE 4% to 12% SDS-PAGE gel (for 1D protein separation) and run for approximately 5 min to electrophorese all proteins into the gel matrix. The entire molecular weight range was then excised in a single gel band and subjected to standardized in-gel reduction, alkylation, and tryptic digestion. Following lyophilization of the extracted peptide mixtures, samples were resuspended in 12 µl of 2% acetonitrile/1% TFA supplemented with 12.5 fmol μl^{-1} yeast ADH. From each sample, 3 µl was removed to create a QC pool sample.

Quantitative LC-MS/MS was performed using 4 µl of each sample, using a nanoACQUITY UPLC system (Waters Corp) coupled to a Thermo Q Exactive HF high resolution, accurate mass tandem mass spectrometer (Thermo) via a nanoelectrospray ionization source. Briefly, the sample was first trapped on a Symmetry C18 20 mm × 180 µm trapping column (5 µl min^{-1} at 99.9/0.1 v/v water/acetonitrile), after which the analytical separation was performed using a 1.8 µm ACQUITY HSS T3 C18 75 µm × 250 mm column (Waters Corp) with a 90-min linear gradient of 5% to 30% acetonitrile with 0.1% formic acid at a flow rate of 400 nl min^{-1} with a column temperature of 55 °C. Data collection on the Q Exactive HF mass spectrometer was performed in a data-dependent acquisition mode with a r = 120,000 (at m/z 200) full MS scan from m/z 375 to 1600 with a target automatic gain control value of 3×10^6 ions followed by 15 MS/MS scans at r = 30,000 (at m/z 200) at a target automatic gain control value of 5×10^4 ions and 45 ms. A 20-s dynamic exclusion was employed to increase depth of coverage. The total analysis cycle time for each sample injection was approximately 2 h.

Following 19 total ultraperformance liquid chromatography–MS/MS analyses (excluding conditioning runs, but including four replicate QC injections), data was imported into Rosetta Elucidator v 4.0 (Rosetta Biosoftware, Inc), and analyses were aligned based on the accurate mass and retention time of detected ions ("features") using PeakTeller algorithm in Elucidator. Relative peptide abundance was calculated based on area under the curve of the selected ion chromatograms of the aligned features across all runs. The MS/MS data were searched against the SwissProt *Mus musculus* database (downloaded in May 2017) with additional proteins, including yeast ADH1, bovine serum albumin, as well as an equal number of reversed-sequence "decoys" for false discovery rate determination. Mascot Distiller and Mascot Server (version 2.5, Matrix Sciences) were utilized to produce fragment ion spectra and to perform the database searches. Database search parameters included fixed modification on Cys (carbamidomethyl) and variable modifications on Meth (oxidation) and Asn and Gln (deamidation). After individual peptide scoring using the PeptideProphet algorithm in Elucidator, the data were annotated at a 1% peptide false discovery rate.

Four microliters of peptide digest (∼30% of each sample) were analyzed by ultraperformance liquid chromatography-tandem mass spectrometry (LC-MS/MS). A QC pool containing an equal mixture of each sample was analyzed first, after every fifth sample, and end of the sample set (four times total). Individual samples were analyzed in a random order. Next, data were imported into Rosetta Elucidator v 4.0 and all LC-MS/MS runs were aligned based on the accurate mass and retention time of detected ions ("features"), which contained MS/MS spectra using PeakTeller algorithm and intensity-scaled based on a robust mean (10%) normalization of the identified features. The overall dataset had 495,664 quantified isotope (peptide) groups. In addition, 330,924 MS/MS spectra were acquired for peptide sequencing by database searching (see Experimental Procedures). Following database searching and peptide scoring using the PeptideProphet algorithm, the data were annotated at a 1% peptide false discovery rate, resulting in identification of 12,497 peptides and 1691 proteins. All proteins were intensity-scaled to levels of HSF1 and subsequent analyses were from these normalized protein levels.

Identification of hit proteins

To remove non-specific proteins or proteins with poor peptide coverage from consideration, only proteins with a

twofold or higher abundance in the HSF1 over the IgG IP ($p < 0.05$) and a ProteinTeller probability of ≥0.80 were used in subsequent analysis. Q7 IgG was used as a negative control for Q7 control HSF1 (unstressed) and Q7 HS HSF1 (heat shock); Q111 IgG was used for Q111 HD. *t* tests were calculated on $\log_2$-transformed data for each of these comparisons using a two-tailed heteroscedastic *t* test in Excel (Microsoft). Of the 1691 proteins identified, 378 (22.4%) passed the aforementioned cutoff requirements.

Generation of 293T HSF1 stable knockdown cells

Stable HSF1 knockdown cells were generated following the second-generation Addgene protocol. Briefly, 293T cells were transfected with psPAX2 (viral packaging), VSVG (viral envelope) plasmids, and either non-targeting sequence shScr plasmid (pLKO.1) or shHSF1 plasmid (TRCN0000007480, Sigma). Transfection was completed with Lipofectamine LTX Reagent (ThermoFisher) following protocol instructions using 21 μg PAX2, 7 μg VSVG, and 28 μg Sigma Mission TRC1 lentiviral shRNA plasmids. Approximately 18 h post transfection, the media was replaced with fresh media. Approximately 48 h post transfection, viral particles were harvested. Supernatant containing lentiviral particles was filtered with a 0.45-μm PES filter to remove any cells from viral production.

Virus-containing, cleared supernatant was applied to 293T cells in standard grown conditions. Twenty-four hours after viral particle addition, media was changed to DMEM containing 0.25 μg/ml puromycin for selection. This concentration of puromycin was determined to be the lowest concentration at which 100% of parental HEK 293T cells would die after 3 days of treatment. After 2 weeks of puromycin selection, no more cell death was observed. shScr and shHSF1 stable knockdowns were analyzed for loss of HSF1 protein to assess knockdown.

Transfection of plasmid DNA and transient siRNA knockdown

Plasmid transfections in 293T cells were completed using Lipofectamine LTX (Invitrogen) according to the manufacturer's protocol (MAN0007822) and were incubated for 24 h before immunoprecipitation experiments. Plasmid transfections in $HSF1^{-/-}$ MEFs with electroporation used the SE Cell Line 4D-Nucleofector (Lonza) with 2×10^6 cells per transfection and 2 μg plasmid DNA according to the manufacture's protocol. Cells were used for immunoprecipitation experiments 24 h after transfection.

Silencing RNAs (siRNA) were obtained from Thermo Fisher Scientific (Silencer Select, assay ID s6950 and s20966 for human HSF1 and CTCF, respectively) and Qiagen (non-targeting siRNA) for negative control scramble (1022076). Transient siRNA knockdowns were completed with Lipofectamine RNAiMAX according to the manufacture's protocol using 25 pmol of siRNA per well of a 6-well plate. The duration of transient knockdown was 48 h before analysis of transcript abundance with qRT-PCR, DNA binding with chromatin immunoprecipitation-qPCR, or immunoblot analysis.

RNA extraction, sequencing, and analysis

RNA was extracted and purified from mammalian cells after 48 h of silencing (four biological replicates for each condition) using RNEasy extraction kit (Qiagen) according to the manufacturer's instructions using QIAshredder columns for homogenization. Library preparation and Illumina sequencing were completed by GeneWiz using the Total RNA process with polyadenylation selection using 2 μg of RNA as input.

Quality of sequencing was assessed with FASTQC and showed samples had sequencing depth of 26 to 36 M reads per sample. Reads were filtered for quality and mapped to the human genome (hg19) using TopHat2 (101). Significant changes in mRNA levels between siRNA treatments were called with DESeq2 (102) with a threshold of $p > 0.001$. Significantly changed genes were broken into high confidence (HC) changes and low confidence (LC) changes using fold change 1.25 as a cutoff. Fold change of HC genes were increased (UpHC) or decreased (DownHC) by 1.25 or more with a p value < 0.001. Fold changes of LC genes were increased (UpLC) or decreased (DownLC) by less than 1.25 with $p < 0.001$. Genes with a low read count (<0.1 normalized reads in all conditions) were categorized as UnExp. Genes with a detectable mRNA expression (minimum of 0.1 normalized reads in any condition) but no significant changes detected with DESeq2 were categorized as unregulated (UnReg). Downstream analysis was conducted only for transcripts with a minimum normalized read count of 10 per gene. Browser images were generated using Integrated Genomics Viewer (103) with density normalized mRNA counts. The raw FASTQ files and density normalized BigWig files can be accessed via Gene Expression Omnibus (GEO; https://www.ncbi.nlm.nih.gov/geo/) using the access code GSE155541.

Protein purification of HSF1 and CTCF

Plasmids were constructed containing STREP-tagged HSF1 or His_6-tagged CTCF (pET-15b, Addgene) and were codon-optimized for bacterial expression. Plasmids were transformed into BL21 (DE3) *E. coli*. Overnight cultures originating from a single colony were diluted 1:100 and grown to log phase at an OD_{600} of ∼0.5 at which point protein expression was induced by addition of 1 mM isopropyl 1-thio-β-D-galactopyranoside overnight at 15 °C. Cells were harvested by centrifugation (10,000 r.c.f., 10 min, 4 °C). For STREP-tagged purification, bacterial cell pellets were lysed with Buffer NP (50 mM NaH_2PO_4, 300 mM NaCl, pH 8.0) supplemented with HALT protease inhibitors (Thermo Fisher). Cells were lysed with sonication on ice (20-s bursts, 80 s total processing time), and lysates were cleared with centrifugation (20,000 r.c.f., 15 min, 4 °C) and applied to a StrepTrap column (GE Heath Sciences) using an Akta Pure FPLC (GE Health Sciences) at a flow rate of 0.25 ml min^{-1}, washed with six column volumes of Buffer NP until the A_{280} was flat, and bound proteins were eluted with Buffer NP supplemented with 2.5 mM desthiobiotin. Fractions containing STREP-HSF1 were analyzed with SDS-PAGE and buffer exchanged using an Amicon Ultra

Centricon (molecular weight cut-off of 10,000 Da) into buffer containing 25 mM HEPES pH 7.5 and 150 mM NaCl. For His-tagged purification, cells were resuspended in NiNTA Lysis Buffer (50 mM HEPES pH 7.5, 300 mM NaCl, 20 mM imidazole HCl) and homogenized with three passages through French pressure cell at >12,000 p.s.i. Cell lysates were cleared with centrifugation as above and incubated with 2 ml of bed volume of Ni-NTA Agarose (Qiagen) for 2 h, 4 °C, rocking. Beads were washed four times with NiNTA Lysis Buffer supplemented with an additional 20 mM imidazole and bound proteins eluted with NiNA Elution Buffer (50 mM HEPES pH 7.5, 300 mM NaCl, 250 mM Imidazole HCl). Fractions were analyzed with SDS-PAGE and immunoblot. His-CTCF was buffer exchanged using an Amicon Ultra Centricon (molecular weight cut-off of 10,000 Da) into buffer containing 25 mM HEPES pH 7.5, 150 mM NaCl, and 1 μM $ZnCl_2$ (104).

HSF1–CTCF in vitro *binding assay*

Binding assays were performed in 1 ml of Buffer NP (50 mM NaH_2PO_4, 300 mM NaCl, pH 8.0) with 5 nM of purified His-CTCF alone or STREP-HSF1 and His-CTCF together. Proteins were incubated for 1 h at 4 °C with rocking and 2 μl of MagStrep type 3 XT resin (IBA) were added and incubated for 30 min at 4 °C with rocking. Beads were washed five times with Buffer NP; interacting proteins were eluted with 25 mM desthiobiotin and analyzed with immunoblot.

Immunoblot analysis

Protein extracts were electrophoresed on 4% to 20% SDS-PAGE and transferred to nitrocellulose membranes (Bio-Rad 0.2 μm) using Transblot Turbo (Bio-Rad) in Tris–glycine buffer (25 nM Tris base, 200 mM glycine) at 25 V. Immunoblots were blocked for 1 h at room temperature with 5% (w/v) milk in PBS supplemented with 0.25% Tween 20 (PBST). Primary antibodies were added to immunoblots (1:1000 in 2.5% milk in PBST) and incubated overnight at 4 °C with rocking. Immunoblots were washed four times, 15 min each in PBST; horseradish peroxidase–conjugated secondary antibodies were added at a 1:5000 dilution in 2.5% milk in PBST; after a final wash (4 times, 15 min each) in PBST, blots were exposed with SuperSignal Chemiluminescent substrate (Thermo Scientific). The primary antibodies used in this study were as follows: anti-HSF1 (Bethyl) (5, 33) and (10H8, Enzo), anti-CTCF (188408 and 37477, Abcam), anti-HA (Y-11, Santa Cruz), anti-FLAG (M2, Sigma), and anti-GAPDH (6C5, Santa Cruz).

Statistical analysis

p-values were obtained using a Student's *t* test comparing means, using two-tailed, unpaired *t* test for samples with heteroscedastic variance. Error bars shown represent mean ± SEM (standard error of the mean). Reported *p*-values correspond to the following: $^{*}p < 0.05$, $^{**}p < 0.01$, $^{***}p < 0.001$; ns, not significant. Pearson correlation and corresponding *p*-value for the correlation was calculated in MATLAB and assessed with Rosner's or Grubb's tests.

Data availability

All data supporting the findings of this publication can be found within the supporting information and the primary publication except those noted here. Fingerprinted proteomics data can be found at MassIVE under the dataset MSV000086045. The raw FASTQ files and density normalized BigWig files can be accessed via Gene Expression Omnibus (GEO; https://www.ncbi.nlm.nih.gov/geo/) using the access code GSE155541.

Acknowledgments—We thank the Duke Proteomics and Metabolomics Shared Resource for their quantitative mass spectrometry services and Duke University School of Medicine for the Core Voucher funding. We acknowledge Bushu Dong for his fantastic scientific advice.

Author contributions—E. T. B. was responsible for project conception, experimental execution, data collection and analysis, and creating and editing this article; A. V. was responsible for computation analysis of RNA-seq data, other computation analyses, aided in project design, and editing this article; M. J. G. was responsible for initial computational analyses; R. G.-P. was responsible for project conception, served as a mentor, aided in project decisions, and editing this article; D. J. T. was responsible for project conception, served as an advisor, aided in project decisions, and editing this article.

Funding and additional information—This work was supported by National Institutes of Health Predoctoral Fellowship F31GM119375 (to E. T. B.), Academy of Finland to (A. V.), and National Institutes of Health R01 A030394 (to D. J. T.). The content is solely the responsibility of the authors and does not necessarily represent the official views of the National Institutes of Health.

Conflict of interest—The authors declare that they have no conflicts of interest with the contents of this article.

Abbreviations—The abbreviations used are: CBY1, chibby family member 1; CTCF, CCCTC-binding factor; DMEM, Dulbecco's modified Eagle's medium; FBS, fetal bovine serum; HC, high confidence; HEK, human embryonic kidney; HD, Huntington's disease; HSE, heat shock element; HSF1, heat shock transcription factor 1; IP, immunoprecipitation; LC, low confidence; mHtt, mutant Htt; NEMF, nuclear export mediator factor; PCA, principal component analysis; polyQ, polyglutamine; QC, quality control; SMC6, structural maintenance of chromosomes protein 6; SNX9, sorting nexin-9; TC-1, thyroid cancer-1; XRCC5, X-ray repair cross complementing 5.

References

1. Gomez-Pastor, R., Burchfiel, E. T., and Thiele, D. J. (2018) Regulation of heat shock transcription factors and their roles in physiology and disease. *Nat. Rev. Mol. Cell Biol.* **19**, 4–19
2. Akerfelt, M., Morimoto, R. I., and Sistonen, L. (2010) Heat shock factors: integrators of cell stress, development and lifespan. *Nat. Rev. Mol. Cell Biol.* **11**, 545–555
3. Vihervaara, A., and Sistonen, L. (2014) HSF1 at a glance. *J. Cell Sci.* **127**, 261–266
4. Nakai, A. (2016) *Heat Shock Factor*, Springer, Japan
5. Neef, D. W., Turski, M. L., and Thiele, D. J. (2010) Modulation of heat shock transcription factor 1 as a therapeutic target for small molecule intervention in neurodegenerative disease. *PLoS Biol.* **8**, e1000291

6. Larson, J. S., Schuetz, T. J., and Kingston, R. E. (1988) Activation *in vitro* of sequence-specific DNA binding by a human regulatory factor. *Nature* **335**, 372–375
7. Shi, Y., Mosser, D. D., and Morimoto, R. I. (1998) Molecular chaperones as HSF1-specific transcriptional repressors. *Genes Dev.* **12**, 654–666
8. Neef, D. W., Jaeger, A. M., Gomez-Pastor, R., Willmund, F., Frydman, J., and Thiele, D. J. (2014) A direct regulatory interaction between chaperonin TRiC and stress-responsive transcription factor HSF1. *Cell Rep.* **9**, 955–966
9. Guo, Y., Guettouche, T., Fenna, M., Boellmann, F., Pratt, W. B., Toft, D. O., Smith, D. F., and Voellmy, R. (2001) Evidence for a mechanism of repression of heat shock factor 1 transcriptional activity by a multichaperone complex. *J. Biol. Chem.* **276**, 45791–45799
10. Krakowiak, J., Zheng, X., Patel, N., Feder, Z. A., Anandhakumar, J., Valerius, K., Gross, D. S., Khalil, A. S., and Pincus, D. (2018) Hsf1 and Hsp70 constitute a two-component feedback loop that regulates the yeast heat shock response. *Elife* **7**, e31668
11. Wang, Y., Gibney, P. A., West, J. D., and Morano, K. A. (2012) The yeast Hsp70 Ssa1 is a sensor for activation of the heat shock response by thiol-reactive compounds. *Mol. Biol. Cell* **23**, 3290–3298
12. Masser, A. E., Ciccarelli, M., and Andréasson, C. (2020) Hsf1 on a leash - controlling the heat shock response by chaperone titration. *Exp. Cell Res.* **396**, 112246
13. Neef, D. W., Jaeger, A. M., and Thiele, D. J. (2013) Genetic selection for constitutively trimerized human HSF1 mutants identifies a role for coiled-coil motifs in DNA binding. *G3 (Bethesda)* **3**, 1315–1324
14. Liu, X. D., Liu, P. C., Santoro, N., and Thiele, D. J. (1997) Conservation of a stress response: human heat shock transcription factors functionally substitute for yeast HSF. *EMBO J.* **16**, 6466–6477
15. Rabindran, S. K., Haroun, R. I., Clos, J., Wisniewski, J., and Wu, C. (1993) Regulation of heat shock factor trimer formation: role of a conserved leucine zipper. *Science* **259**, 230–234
16. Zuo, J., Baler, R., Dahl, G., and Voellmy, R. (1994) Activation of the DNA-binding ability of human heat shock transcription factor 1 may involve the transition from an intramolecular to an intermolecular triple-stranded coiled-coil structure. *Mol. Cell Biol.* **14**, 7557–7568
17. Hentze, N., Le Breton, L., Wiesner, J., Kempf, G., and Mayer, M. P. (2016) Molecular mechanism of thermosensory function of human heat shock transcription factor Hsf1. *Elife* **5**, e11576
18. Scherz-Shouval, R., Santagata, S., Mendillo, M. L., Sholl, L. M., Ben-Aharon, I., Beck, A. H., Dias-Santagata, D., Koeva, M., Stemmer, S. M., Whitesell, L., and Lindquist, S. (2014) The reprogramming of tumor stroma by HSF1 is a potent enabler of malignancy. *Cell* **158**, 564–578
19. Mendillo, M. L., Santagata, S., Koeva, M., Bell, G. W., Hu, R., Tamimi, R. M., Fraenkel, E., Ince, T. A., Whitesell, L., and Lindquist, S. (2012) HSF1 drives a transcriptional program distinct from heat shock to support highly malignant human cancers. *Cell* **150**, 549–562
20. Cahill, C. M., Waterman, W. R., Xie, Y., Auron, P. E., and Calderwood, S. K. (1996) Transcriptional repression of the prointerleukin 1beta gene by heat shock factor 1. *J. Biol. Chem.* **271**, 24874–24879
21. Singh, I. S., He, J. R., Calderwood, S., and Hasday, J. D. (2002) A high affinity HSF-1 binding site in the 5'-untranslated region of the murine tumor necrosis factor-alpha gene is a transcriptional repressor. *J. Biol. Chem.* **277**, 4981–4988
22. Xie, Y., Chen, C., Stevenson, M. A., Auron, P. E., and Calderwood, S. K. (2002) Heat shock factor 1 represses transcription of the IL-1beta gene through physical interaction with the nuclear factor of interleukin 6. *J. Biol. Chem.* **277**, 11802–11810
23. Inouye, S., Fujimoto, M., Nakamura, T., Takaki, E., Hayashida, N., Hai, T., and Nakai, A. (2007) Heat shock transcription factor 1 opens chromatin structure of interleukin-6 promoter to facilitate binding of an activator or a repressor. *J. Biol. Chem.* **282**, 33210–33217
24. Takii, R., Fujimoto, M., Tan, K., Takaki, E., Hayashida, N., Nakato, R., Shirahige, K., and Nakai, A. (2015) ATF1 modulates the heat shock response by regulating the stress-inducible heat shock factor 1 transcription complex. *Mol. Cell Biol.* **35**, 11–25
25. Vihervaara, A., Sergelius, C., Vasara, J., Blom, M. A., Elsing, A. N., Roos-Mattjus, P., and Sistonen, L. (2013) Transcriptional response to stress in the dynamic chromatin environment of cycling and mitotic cells. *Proc. Natl. Acad. Sci. U. S. A.* **110**, E3388–E3397
26. Vihervaara, A., Mahat, D. B., Guertin, M. J., Chu, T., Danko, C. G., Lis, J. T., and Sistonen, L. (2017) Transcriptional response to stress is pre-wired by promoter and enhancer architecture. *Nat. Commun.* **8**, 255
27. Mahat, D. B., Salamanca, H. H., Duarte, F. M., Danko, C. G., and Lis, J. T. (2016) Mammalian heat shock response and mechanisms underlying its genome-wide transcriptional regulation. *Mol. Cell* **62**, 63–78
28. Riva, L., Koeva, M., Yildirim, F., Pirhaji, L., Dinesh, D., Mazor, T., Duennwald, M. L., and Fraenkel, E. (2012) Poly-glutamine expanded huntingtin dramatically alters the genome wide binding of HSF1. *J. Huntingtons Dis.* **1**, 33–45
29. Hay, D. G., Sathasivam, K., Tobaben, S., Stahl, B., Marber, M., Mestril, R., Mahal, A., Smith, D. L., Woodman, B., and Bates, G. P. (2004) Progressive decrease in chaperone protein levels in a mouse model of Huntington's disease and induction of stress proteins as a therapeutic approach. *Hum. Mol. Genet.* **13**, 1389–1405
30. Labbadia, J., Cunliffe, H., Weiss, A., Katsyuba, E., Sathasivam, K., Seredenina, T., Woodman, B., Moussaoui, S., Frentzel, S., Luthi-Carter, R., Paganetti, P., and Bates, G. P. (2011) Altered chromatin architecture underlies progressive impairment of the heat shock response in mouse models of Huntington disease. *J. Clin. Invest.* **121**, 3306–3319
31. Chafekar, S. M., and Duennwald, M. L. (2012) Impaired heat shock response in cells expressing full-length polyglutamine-expanded huntingtin. *PLoS One* **7**, e37929
32. Hodges, A., Strand, A. D., Aragaki, A. K., Kuhn, A., Sengstag, T., Hughes, G., Elliston, L. A., Hartog, C., Goldstein, D. R., Thu, D., Hollingsworth, Z. R., Collin, F., Synek, B., Holmans, P. A., Young, A. B., *et al.* (2006) Regional and cellular gene expression changes in human Huntington's disease brain. *Hum. Mol. Genet.* **15**, 965–977
33. Gomez-Pastor, R., Burchfiel, E. T., Neef, D. W., Jaeger, A. M., Cabiscol, E., McKinstry, S. U., Doss, A., Aballay, A., Lo, D. C., Akimov, S. S., Ross, C. A., Eroglu, C., and Thiele, D. J. (2017) Abnormal degradation of the neuronal stress-protective transcription factor HSF1 in Huntington's disease. *Nat. Commun.* **8**, 14405
34. A novel gene containing a trinucleotide repeat that is expanded and unstable on Huntington's disease chromosomes. The Huntington's Disease Collaborative Research Group. *Cell* **72**, (1993), 971–983
35. Landles, C., and Bates, G. P. (2004) Huntingtin and the molecular pathogenesis of Huntington's disease. Fourth in molecular medicine review series. *EMBO Rep.* **5**, 958–963
36. La Spada, A. R., Weydt, P., and Pineda, V. V. (2011) Frontiers in neuroscience Huntington's disease pathogenesis: mechanisms and pathways. In: Lo, D. C., Hughes, R. E., eds. *Neurobiology of Huntington's Disease: Applications to Drug Discovery*, CRC Press/Taylor & Francis Llc., Boca Raton, FL: 29–54
37. Chan, H. Y., Warrick, J. M., Gray, B., Paulson, H. L., and Bonini, N. M. (2000) Mechanisms of chaperone suppression of polyglutamine disease: selectivity, synergy and modulation of protein solubility in Drosophila. *Hum. Mol. Genet.* **9**, 2811–2820
38. Warrick, J. M., Chan, H. Y., Gray, B., Chai, Y., Paulson, H. L., and Bonini, N. M. (1999) Suppression of polyglutamine-mediated neurodegeneration in Drosophila by the molecular chaperone HSP70. *Nat. Genet.* **23**, 425–428
39. Wyttenbach, A., Carmichael, J., Swartz, J., Furlong, R. A., Narain, Y., Rankin, J., and Rubinsztein, D. C. (2000) Effects of heat shock, heat shock protein 40 (HDJ-2), and proteasome inhibition on protein aggregation in cellular models of Huntington's disease. *Proc. Natl. Acad. Sci. U. S. A.* **97**, 2898–2903
40. Rubinsztein, D. C., Gestwicki, J. E., Murphy, L. O., and Klionsky, D. J. (2007) Potential therapeutic applications of autophagy. *Nat. Rev. Drug Discov.* **6**, 304–312
41. Behrends, C., Langer, C. A., Boteva, R., Bottcher, U. M., Stemp, M. J., Schaffar, G., Rao, B. V., Giese, A., Kretzschmar, H., Siegers, K., and Hartl, F. U. (2006) Chaperonin TRiC promotes the assembly of polyQ expansion proteins into nontoxic oligomers. *Mol. Cell* **23**, 887–897
42. Balch, W. E., Morimoto, R. I., Dillin, A., and Kelly, J. W. (2008) Adapting proteostasis for disease intervention. *Science* **319**, 916–919

43. Bailey, C. K., Andriola, I. F., Kampinga, H. H., and Merry, D. E. (2002) Molecular chaperones enhance the degradation of expanded polyglutamine repeat androgen receptor in a cellular model of spinal and bulbar muscular atrophy. *Hum. Mol. Genet.* **11**, 515–523
44. West, J. D., Wang, Y., and Morano, K. A. (2012) Small molecule activators of the heat shock response: chemical properties, molecular targets, and therapeutic promise. *Chem. Res. Toxicol.* **25**, 2036–2053
45. Mun, G. I., Choi, E., Lee, Y., and Lee, Y. S. (2020) Decreased expression of FBXW7 by ERK1/2 activation in drug-resistant cancer cells confers transcriptional activation of MDR1 by suppression of ubiquitin degradation of HSF1. *Cell Death Dis.* **11**, 395
46. Kourtis, N., Moubarak, R. S., Aranda, O., Lui, K., Aydin, I. T., Trimarchi, T., Darvishian, F., Salvaggio, C., Zhong, J., Bhatt, K., Chen, E. I., Celebi, J. T., Lazaris, C., Tsirigos, A., Osman, I., *et al.* (2015) FBXW7 modulates cellular stress response and metastatic potential through HSF1 post-translational modification. *Nat. Cell Biol.* **17**, 322–332
47. Kourtis, N., Strikoudis, A., and Aifantis, I. (2015) Emerging roles for the FBXW7 ubiquitin ligase in leukemia and beyond. *Curr. Opin. Cell Biol.* **37**, 28–34
48. Sailo, B. L., Banik, K., Girisa, S., Bordoloi, D., Fan, L., Halim, C. E., Wang, H., Kumar, A. P., Zheng, D., Mao, X., Sethi, G., and Kunnumakkara, A. B. (2019) FBXW7 in cancer: what has been unraveled thus far? *Cancers (Basel)* **11**
49. Jin, Y. H., Ahn, S. G., and Kim, S. A. (2015) BAG3 affects the nucleocytoplasmic shuttling of HSF1 upon heat stress. *Biochem. Biophys. Res. Commun.* **464**, 561–567
50. Fujimoto, M., Takaki, E., Takii, R., Tan, K., Prakasam, R., Hayashida, N., Iemura, S., Natsume, T., and Nakai, A. (2012) RPA assists HSF1 access to nucleosomal DNA by recruiting histone chaperone FACT. *Mol. Cell* **48**, 182–194
51. Tan, K., Fujimoto, M., Takii, R., Takaki, E., Hayashida, N., and Nakai, A. (2015) Mitochondrial SSBP1 protects cells from proteotoxic stresses by potentiating stress-induced HSF1 transcriptional activity. *Nat. Commun.* **6**, 6580
52. Xie, Y., Zhong, R., Chen, C., and Calderwood, S. K. (2003) Heat shock factor 1 contains two functional domains that mediate transcriptional repression of the c-fos and c-fms genes. *J. Biol. Chem.* **278**, 4687–4698
53. Huang, J., Nueda, A., Yoo, S., and Dynan, W. S. (1997) Heat shock transcription factor 1 binds selectively *in vitro* to Ku protein and the catalytic subunit of the DNA-dependent protein kinase. *J. Biol. Chem.* **272**, 26009–26016
54. Fujimoto, M., Takii, R., Takaki, E., Katiyar, A., Nakato, R., Shirahige, K., and Nakai, A. (2017) The HSF1-PARP13-PARP1 complex facilitates DNA repair and promotes mammary tumorigenesis. *Nat. Commun.* **8**, 1638
55. Minsky, N., and Roeder, R. G. (2015) Direct link between metabolic regulation and the heat-shock response through the transcriptional regulator PGC-1α. *Proc. Natl. Acad. Sci. U. S. A.* **112**, E5669–E5678
56. Katiyar, A., Fujimoto, M., Tan, K., Kurashima, A., Srivastava, P., Okada, M., Takii, R., and Nakai, A. (2020) HSF1 is required for induction of mitochondrial chaperones during the mitochondrial unfolded protein response. *FEBS Open Bio.* **10**, 1135–1148
57. Trettel, F., Rigamonti, D., Hilditch-Maguire, P., Wheeler, V. C., Sharp, A. H., Persichetti, F., Cattaneo, E., and MacDonald, M. E. (2000) Dominant phenotypes produced by the HD mutation in STHdh(Q111) striatal cells. *Hum. Mol. Genet.* **9**, 2799–2809
58. Zuo, J., Rungger, D., and Voellmy, R. (1995) Multiple layers of regulation of human heat shock transcription factor 1. *Mol. Cell Biol.* **15**, 4319–4330
59. Kim, E., Wang, B., Sastry, N., Masliah, E., Nelson, P. T., Cai, H., and Liao, F. F. (2016) NEDD4-mediated HSF1 degradation underlies α-synucleinopathy. *Hum. Mol. Genet.* **25**, 211–222
60. Beer, L. A., Tang, H. Y., Sriswasdi, S., Barnhart, K. T., and Speicher, D. W. (2011) Systematic discovery of ectopic pregnancy serum biomarkers using 3-D protein profiling coupled with label-free quantitation. *J. Proteome Res.* **10**, 1126–1138
61. Taipale, M., Tucker, G., Peng, J., Krykbaeva, I., Lin, Z. Y., Larsen, B., Choi, H., Berger, B., Gingras, A. C., and Lindquist, S. (2014) A quantitative chaperone interaction network reveals the architecture of cellular protein homeostasis pathways. *Cell* **158**, 434–448
62. Chen, Y., Yang, L. N., Cheng, L., Tu, S., Guo, S. J., Le, H. Y., Xiong, Q., Mo, R., Li, C. Y., Jeong, J. S., Jiang, L., Blackshaw, S., Bi, L. J., Zhu, H., Tao, S. C., *et al.* (2013) Bcl2-associated athanogene 3 interactome analysis reveals a new role in modulating proteasome activity. *Mol. Cell Proteomics* **12**, 2804–2819
63. Boldt, K., van Reeuwijk, J., Lu, Q., Koutroumpas, K., Nguyen, T. M., Texier, Y., van Beersum, S. E., Horn, N., Willer, J. R., Mans, D. A., Dougherty, G., Lamers, I. J., Coene, K. L., Arts, H. H., Betts, M. J., *et al.* (2016) An organelle-specific protein landscape identifies novel diseases and molecular mechanisms. *Nat. Commun.* **7**, 11491
64. Lee, Y. J., Lee, H. J., Lee, J. S., Jeoung, D., Kang, C. M., Bae, S., Lee, S. J., Kwon, S. H., Kang, D., and Lee, Y. S. (2008) A novel function for HSF1-induced mitotic exit failure and genomic instability through direct interaction between HSF1 and Cdc20. *Oncogene* **27**, 2999–3009
65. Sullivan, E. K., Weirich, C. S., Guyon, J. R., Sif, S., and Kingston, R. E. (2001) Transcriptional activation domains of human heat shock factor 1 recruit human SWI/SNF. *Mol. Cell Biol.* **21**, 5826–5837
66. Gorynia, S., Bandeiras, T. M., Pinho, F. G., McVey, C. E., Vonrhein, C., Round, A., Svergun, D. I., Donner, P., Matias, P. M., and Carrondo, M. A. (2011) Structural and functional insights into a dodecameric molecular machine - the RuvBL1/RuvBL2 complex. *J. Struct. Biol.* **176**, 279–291
67. Zlatanova, J., and Caiafa, P. (2009) CTCF and its protein partners: divide and rule? *J. Cell Sci.* **122**, 1275–1284
68. Lutz, M., Burke, L. J., Barreto, G., Goeman, F., Greb, H., Arnold, R., Schultheiss, H., Brehm, A., Kouzarides, T., Lobanenkov, V., and Renkawitz, R. (2000) Transcriptional repression by the insulator protein CTCF involves histone deacetylases. *Nucleic Acids Res.* **28**, 1707–1713
69. Zuin, J., Dixon, J. R., van der Reijden, M. I., Ye, Z., Kolovos, P., Brouwer, R. W., van de Corput, M. P., van de Werken, H. J., Knoch, T. A., van, I. W. F., Grosveld, F. G., Ren, B., and Wendt, K. S. (2014) Cohesin and CTCF differentially affect chromatin architecture and gene expression in human cells. *Proc. Natl. Acad. Sci. U. S. A.* **111**, 996–1001
70. Ostling, P., Björk, J. K., Roos-Mattjus, P., Mezger, V., and Sistonen, L. (2007) Heat shock factor 2 (HSF2) contributes to inducible expression of hsp genes through interplay with HSF1. *J. Biol. Chem.* **282**, 7077–7086
71. Inouye, S., Katsuki, K., Izu, H., Fujimoto, M., Sugahara, K., Yamada, S., Shinkai, Y., Oka, Y., Katoh, Y., and Nakai, A. (2003) Activation of heat shock genes is not necessary for protection by heat shock transcription factor 1 against cell death due to a single exposure to high temperatures. *Mol. Cell Biol.* **23**, 5882–5895
72. Jaeger, A., Pemble, C., Sistonen, L., and Thiele, D. (2016) Structures of HSF2 reveal mechanisms for differential regulation of human heat-shock factors. *Nat. Struct. Mol. Biol.* **23**, 147–154
73. Littlefield, O., and Nelson, H. C. (1999) A new use for the 'wing' of the 'winged' helix-turn-helix motif in the HSF-DNA cocrystal. *Nat. Struct. Biol.* **6**, 464–470
74. Ray, J., Munn, P. R., Vihervaara, A., Lewis, J. J., Ozer, A., Danko, C. G., and Lis, J. T. (2019) Chromatin conformation remains stable upon extensive transcriptional changes driven by heat shock. *Proc. Natl. Acad. Sci. U. S. A.* **116**, 19431–19439
75. Ritossa, F. (1962) A new puffing pattern induced by temperature shock and DNP in drosophila. *Experientia* **18**, 571–573
76. Jiang, Y. Q., Wang, X. L., Cao, X. H., Ye, Z. Y., Li, L., and Cai, W. Q. (2013) Increased heat shock transcription factor 1 in the cerebellum reverses the deficiency of Purkinje cells in Alzheimer's disease. *Brain Res.* **1519**, 105–111
77. Goetzl, E. J., Boxer, A., Schwartz, J. B., Abner, E. L., Petersen, R. C., Miller, B. L., Carlson, O. D., Mustapic, M., and Kapogiannis, D. (2015) Low neural exosomal levels of cellular survival factors in Alzheimer's disease. *Ann. Clin. Transl. Neurol.* **2**, 769–773
78. Pierce, A., Podlutskaya, N., Halloran, J. J., Hussong, S. A., Lin, P. Y., Burbank, R., Hart, M. J., and Galvan, V. (2013) Over-expression of heat shock factor 1 phenocopies the effect of chronic inhibition of TOR by rapamycin and is sufficient to ameliorate Alzheimer's-like deficits in mice modeling the disease. *J. Neurochem.* **124**, 880–893

79. Runne, H., Régulier, E., Kuhn, A., Zala, D., Gokce, O., Perrin, V., Sick, B., Aebischer, P., Déglon, N., and Luthi-Carter, R. (2008) Dysregulation of gene expression in primary neuron models of Huntington's disease shows that polyglutamine-related effects on the striatal transcriptome may not be dependent on brain circuitry. *J. Neurosci.* **28**, 9723–9731
80. Gall, C., Xu, H., Brickenden, A., Ai, X., and Choy, W. Y. (2007) The intrinsically disordered TC-1 interacts with Chibby via regions with high helical propensity. *Protein Sci.* **16**, 2510–2518
81. Massey, T. H., and Jones, L. (2018) The central role of DNA damage and repair in CAG repeat diseases. *Dis. Model Mech.* **11**, dmm031930
82. McMurray, C. T. (2008) Hijacking of the mismatch repair system to cause CAG expansion and cell death in neurodegenerative disease. *DNA Repair (Amst)* **7**, 1121–1134
83. Brandman, O., Stewart-Ornstein, J., Wong, D., Larson, A., Williams, C. C., Li, G. W., Zhou, S., King, D., Shen, P. S., Weibezahn, J., Dunn, J. G., Rouskin, S., Inada, T., Frost, A., and Weissman, J. S. (2012) A ribosome-bound quality control complex triggers degradation of nascent peptides and signals translation stress. *Cell* **151**, 1042–1054
84. Kijima, T., Prince, T. L., Tigue, M. L., Yim, K. H., Schwartz, H., Beebe, K., Lee, S., Budzynski, M. A., Williams, H., Trepel, J. B., Sistonen, L., Calderwood, S., and Neckers, L. (2018) HSP90 inhibitors disrupt a transient HSP90-HSF1 interaction and identify a noncanonical model of HSP90-mediated HSF1 regulation. *Sci. Rep.* **8**, 6976
85. Kmiecik, S. W., Le Breton, L., and Mayer, M. P. (2020) Feedback regulation of heat shock factor 1 (Hsf1) activity by Hsp70-mediated trimer unzipping and dissociation from DNA. *EMBO J.* **39**, e104096
86. Zheng, X., and Pincus, D. (2017) Serial immunoprecipitation of 3xFLAG/V5-tagged yeast proteins to identify specific interactions with chaperone proteins. *Bio. Protoc.* **7**, e2348
87. Klenova, E. M., Nicolas, R. H., Paterson, H. F., Carne, A. F., Heath, C. M., Goodwin, G. H., Neiman, P. E., and Lobanenkov, V. V. (1993) CTCF, a conserved nuclear factor required for optimal transcriptional activity of the chicken c-myc gene, is an 11-Zn-finger protein differentially expressed in multiple forms. *Mol. Cell Biol.* **13**, 7612–7624
88. Takii, R., Fujimoto, M., Matsumoto, M., Srivastava, P., Katiyar, A., Nakayama, K. I., and Nakai, A. (2019) The pericentromeric protein shugoshin 2 cooperates with HSF1 in heat shock response and RNA Pol II recruitment. *EMBO J.* **38**, e102566
89. Ong, C. T., and Corces, V. G. (2014) CTCF: an architectural protein bridging genome topology and function. *Nat. Rev. Genet.* **15**, 234–246
90. Chowdhary, S., Kainth, A. S., Pincus, D., and Gross, D. S. (2019) Heat shock factor 1 drives intergenic association of its target gene loci upon heat shock. *Cell Rep.* **26**, 18–28.e15
91. Kim, S., and Gross, D. S. (2013) Mediator recruitment to heat shock genes requires dual Hsf1 activation domains and mediator tail subunits Med15 and Med16. *J. Biol. Chem.* **288**, 12197–12213
92. Felsenfeld, G., Burgess-Beusse, B., Farrell, C., Gaszner, M., Ghirlando, R., Huang, S., Jin, C., Litt, M., Magdinier, F., Mutskov, V., Nakatani, Y., Tagami, H., West, A., and Yusufzai, T. (2004) Chromatin boundaries and chromatin domains. *Cold Spring Harb. Symp. Quant. Biol.* **69**, 245–250
93. Splinter, E., Heath, H., Kooren, J., Palstra, R. J., Klous, P., Grosveld, F., Galjart, N., and de Laat, W. (2006) CTCF mediates long-range chromatin looping and local histone modification in the beta-globin locus. *Genes Dev.* **20**, 2349–2354
94. Guertin, M. J., and Lis, J. T. (2010) Chromatin landscape dictates HSF binding to target DNA elements. *PLoS Genet.* **6**, e1001114
95. Corey, L. L., Weirich, C. S., Benjamin, I. J., and Kingston, R. E. (2003) Localized recruitment of a chromatin-remodeling activity by an activator *in vivo* drives transcriptional elongation. *Genes Dev.* **17**, 1392–1401
96. Liu, Z., Scannell, D. R., Eisen, M. B., and Tjian, R. (2011) Control of embryonic stem cell lineage commitment by core promoter factor, TAF3. *Cell* **146**, 720–731
97. Shopland, L. S., Hirayoshi, K., Fernandes, M., and Lis, J. T. (1995) HSF access to heat shock elements *in vivo* depends critically on promoter architecture defined by GAGA factor, TFIID, and RNA polymerase II binding sites. *Genes Dev.* **9**, 2756–2769
98. Fernández-Nogales, M., Cabrera, J. R., Santos-Galindo, M., Hoozemans, J. J., Ferrer, I., Rozemuller, A. J., Hernández, F., Avila, J., and Lucas, J. J. (2014) Huntington's disease is a four-repeat tauopathy with tau nuclear rods. *Nat. Med.* **20**, 881–885
99. Vuono, R., Winder-Rhodes, S., de Silva, R., Cisbani, G., Drouin-Ouellet, J., REGISTRY Investigators of the European Huntington's Disease Network, Spillantini, M. G., Cicchetti, F., and Barker, R. A. (2015) The role of tau in the pathological process and clinical expression of Huntington's disease. *Brain* **138**, 1907–1918
100. Wood, H. (2015) Neurodegenerative disease: tau is linked to cognitive decline in Huntington disease. *Nat. Rev. Neurol.* **11**, 310
101. Kim, D., Pertea, G., Trapnell, C., Pimentel, H., Kelley, R., and Salzberg, S. L. (2013) TopHat2: accurate alignment of transcriptomes in the presence of insertions, deletions and gene fusions. *Genome Biol.* **14**, R36
102. Love, M. I., Huber, W., and Anders, S. (2014) Moderated estimation of fold change and dispersion for RNA-seq data with DESeq2. *Genome Biol.* **15**, 550
103. Thorvaldsdóttir, H., Robinson, J. T., and Mesirov, J. P. (2013) Integrative Genomics Viewer (IGV): high-performance genomics data visualization and exploration. *Brief Bioinform.* **14**, 178–192
104. Voráčková, I., Suchanová, S., Ulbrich, P., Diehl, W. E., and Ruml, T. (2011) Purification of proteins containing zinc finger domains using immobilized metal ion affinity chromatography. *Protein Expr. Purif.* **79**, 88–95
105. Zhang, L., Hu, Z., Zhang, Y., Huang, J., Yang, X., and Wang, J. (2019) Proteomics analysis of proteins interacting with heat shock factor 1 in squamous cell carcinoma of the cervix. *Oncol. Lett.* **18**, 2568–2575
106. Kovács, D., Sigmond, T., Hotzi, B., Bohár, B., Fazekas, D., Deák, V., Vellai, T., and Barna, J. (2019) HSF1Base: a comprehensive database of HSF1 (heat shock factor 1) target genes. *Int. J. Mol. Sci.* **20**, 5815

Since **Eileen T. Burchfiel** first learned about HSF1 and its intricately regulated activation–attenuation cycle, she was fascinated by the largely unexplored regulation of HSF1 by protein–protein interactions. There remain many unanswered questions about HSF1 biology, but this study provides new insights to the HSF1 protein interactome in stress and disease. After concluding this work, Eileen began as a scientist at Remix Therapeutics, an innovative biotech startup in Cambridge, Massachusetts, that focuses on modulation of RNA processing for therapeutic development.